Kurbanov F, Tanaka Y, Mizokami M.	Geographical and genetic diversity of the human hepatitis B virus.	Hepatol Res.	40(1)	14-30.	2010.
Tatematsu K, Tanaka Y, Kurbanov F, Sugauchi F, Mano S, Maeshiro T, Nakayoshi T, Wakuta M, Miyakawa Y, Mizokami M.	A genetic variant of hepatitis B virus divergent from known human and ape genotypes isolated from a Japanese patient and provisionally assigned to new genotype J.	J Virol.	83(20)	10538-10547.	2009.
.Khan A, Tanaka Y, Azam Z, Abbas Z, Kurbanov F, Saleem U, Hamid S, Jafri W, Mizokami M.	Epidemic spread of hepatitis C virus genotype 3a and relation to high incidence of hepatocellular carcinoma in Pakistan.	J Med Virol.	81(7)	1189-1197.	2009.
Elkady A, Tanaka Y, Kurbanov F, Sugauchi F, Sugiyama M, Khan A, Sayed D, Moustafa G, Abdel-Hameed AR, Mizokami M.	Genetic variability of hepatitis C virus in South Egypt and its possible clinical implication.	J Med Virol.	81(6)	1015-1023.	2009.

研究分担者　中西　真

雑誌

発表者氏名	論文タイトル名	発表誌名	巻号	ページ	出版年
Sato S, Takahashi S, Asamoto M, Nakanishi M, Wakita T, Ogura Y, Yatabe Y, Shirai T.	Histone H1 expression in human prostate cancer tissues and cell lines.	Pathol Int.	62	84-92	2012
Delhase M, Kim SY, Lee H, Naiki-Ito A, Chen Y, Ahn ER, Murata K, Kim SJ, Lautsch N, Kobayashi KS, Shirai T, Karin M, Nakanishi M.	TANK-binding kinase 1 (TBK1) controls cell survival through PAI-2/serpinB2 and transglutaminase 2.	Proc Natl Acad Sci U S A.	109	177-86	2012

Ogawa K, Murasaki T, Sugiura S, Nakanishi M, Shirai T.	Organ differences in the impact of p27(kip1) deficiency on carcinogenesis induced by N-methyl-N-nitrosourea.	J Appl Toxicol.	In press		2011
Sugiyama M, Tanaka Y, Wakita T, Nakanishi M, Mizokami M.	Genetic variation of the IL-28B promoter affecting gene expression.	PLoS One			2011
Nakanishi M.	Cell cycle	Rinsho Ketsueki.	52	1660-8	2011
Sugiyama M, Inui A, Shin-I T, Komatsu H, Mukaide M, Masaki N, Murata K, Ito K, Nakanishi M, Fujisawa T, Mizokami M.	Easy-to-use phylogenetic analysis system for hepatitis B virus infection.	Hepatol Res.	41	936-945	2011
Harada N, Watanabe Y, Yoshimura Y, Sakumoto H, Makishima F, Tsuchiya M, Nakanishi K, Nakanishi M, Aoki Y.	Identification of a checkpoint modulator with synthetic lethality to p53 mutants.	Anticancer Drugs.	22	986-94	2011
Matsuyama M, Goto H, Kasahara K, Kawakami Y, Nakanishi M, Kiyono T, Goshima N, Inagaki M.	Nuclear Chk1 prevents premature mitotic entry.	J Cell Sci.	124	2113-9	2011
Mizutani E, Suzumori N, Ozaki Y, Oseto K, Yamada-Namikawa C, Nakanishi M, Sugiura-Ogasawara M.	SYCP3 mutation may not be associated with recurrent miscarriage caused by aneuploidy.	Hum Reprod.	26	1259-66	2011
Sugiyama M, Tanaka Y, Nakanishi M, Mizokami M.	Novel findings for the development of drug therapy for various liver diseases: Genetic variation in IL-28B is associated with response to the therapy for chronic hepatitis C.	J Pharmacol Sci.	115	263-9	2011

Shimada, M., Haruta, M., Niida, H., Sawamoto, K., and Nakanishi, M.	PP1g is a phosphatase responsible for dephosphorylation of histone H3 at threonine 11 after DNA damage.	EMBO rep.	11	883-889	2010
Niida, H., Shimada, M., Murakami, H., and Nakanishi, M.	Mechanisms of dNTP supply that play an essential role in maintaining genome integrity in eukaryotic cells.	Cancer Sci.	101	2505-2509	2010
Niida, H., Murata, K., Shimada, M., Ogawa, K., Ohta, K., Suzuki, K., Fujigaki, H., Khaw, A.K., Banerjee, B., Hande, P.M., Miyamoto, T., Miyoshi, I., Shirai, T., Motoyama, N., Delhase, M., Appella, E., and Nakanishi, M.	Cooperative functions of Chk1 and Chk2 reduce tumor suscepti bility in vivo.	EMBO J.	29	3558-3570	2010
Murakami, H., Aiba, H., Nakanishi, M., and Murakami-Tonami, Y.	Regulation of yeast forkhead transcription factors and FoxM1 by cyclin-dependent and polo-like kinases.	Cell Cycle	9	3233-3242	2010
Sakai, S., Ohoka, N., Onozaki, K., Kitagawa, M., Nakanishi, M., and Hayashi, H.	Dual mode of regulation of cell division cycle 25A protein by TRB3.	Biol Pharm Bull.	33	1112-1116	2010
Niida, H., Katsuno, Y., Sengoku, M., Shimada, M., Yukawa, M., Ikura, M., Ikura, T., Kohno, K., Shima, H., Suzuki, H., Tashiro, S., and *Nakanishi, M.	Essential role of Tip60-dependent recruitment of ribonucleotide reductase at DNA damage sites in DNA repair during G1 phase.	Genes and Dev.	24	333-338	2010
Ohoka, N., Sakai, S., Onozaki, K., Nakanishi, M., and Hayashi, H.	Anaphase promoting complex/cyclosome-cdh1 mediates the ubiquitination and degradation of TRB3.	Biochem. Biophys. Res. Commun.	392	289-294	2010

Nakanishi, M., Katsuno, Y., Niida, H., Murakami, H., and Shimada, M.	Chk1-cycline A/Cdk1 axis regulatesorigin firing programs in mammals.	Chromosomal Res.	18	103-113	2010
Nakanishi, M., Niida, H., Murakami, H., and Shimada, M.	DNA damage responses in skin biology-Implications in tumor prevention and aging acceleration.	J Dermatol Sci.	56	76-81	2009
Shimada,M.,Yamamoto,A.,Murakami-Tonami, Y., Nakanishi, M., Yoshida, T., Aiba, H., and Murakami, H.	Casein kinase II is required for the spindle assembly checkpoint by regulating Mad2p in fission yeast.	Biochem. Biophys. Res. Commun.	388	529-532	2009
Zineldeen, D.H., Shimada, M., Niida, H., Katsuno, Y., and Nakanishi, M.	Ptpcd-1 is a novel cell cycle related phosphatase that regulates centriole duplication and cytokinesis.	Biochem. Biophys. Res. Commun.	380	460-466	2009
Nishizuka, M., Kishimoto, K., Kato, A., Ikawa, M., Okabe, M., Sato, R., Niida, H., Nakanishi, M., Osada, S., and Imagawa, M.	Disruption of the novel gene fad14 causes rapid postnatal death and attenuation of cell proliferation, adhesion, spreading and migration.	Exp. Cell Res.	315	809-819	2009
Katsuno, Y., Suzuki, A., Sugimura, K., Okumura, K., Zineldeen, D.H., Shimada, M., Niida, H., Mizuno, T., Hanaoka, F., and Nakanishi, M.	Cyclin A-Cdk1 regulates the origin firing program in mammalian cells.	Proc. Natl. Acad. Sci.	106	3184-3189	2009

研究分担者　水口　裕之

雑誌

発表者氏名	論文タイトル名	発表誌名	巻号	ページ	出版年
Kawabata K., Takayama K., Nagamoto Y., Saldon M.S., Higuchi M., Mizuguchi H.	Endodermal and hepatic differentiation from human embryonic stem cells and human induced pluripotent stem cells.	J. Stem Cell Res. Ther.	印刷中		

Kawabata K., Inamura M., Mizuguchi H.	Efficient hepatic differentiation of human iPS cells by gene transfer.	Methods. Mol. Biol.	326	115-124	2012
Takayama K., Inamura M., Kawabata K., Katayama K., Higuchi M., Tashiro K., Nonaka A., Sakurai F., Hayakawa T., Furue MK., Mizuguchi H.	Efficient generation of functional hepatocytes from human embryonic stem cells and induced pluripotent stem cells by HNF4α transduction.	Mol.Ther.	20	127-137	2012
Yoshida T., Takayama K., Kondoh M., Sakurai F., Tani H., Sakamoto N., Matsuura Y., Mizuguchi H., Yagi K.	Use of human hepatocyte-like cells derived from induced pluripotent stem cells as a model for hepatocytes in hepatitis C virus infection.	Biochem. Biophys. Res. Commun.	416	119-124	2011
Takayama K., Inamura M., Kawabata K., Tashiro K., Katayama K., Hayakawa T., Furue MK., Mizuguchi H.	Efficient and selective generation of two distinct endoderm lineages from human ES and iPS cells by differentiation stage-specific SOX17 transduction.	PLoS One	6	e21780	2011
Inamura M, Kawabata K, Takayama K, Tashiro K, Sakurai F, Katayama K, Toyoda M, Akutsu H, Miyagawa Y, Okita H, Kiyokawa N, Umezawa A, Hayakawa T, Furue MK, Mizuguchi H.	Efficient generation of hepatoblasts from human ES cells and iPS cells by transient overexpression of homeobox gene HEX.	Mol. Ther.	19	400-407	2011
Tashiro K, Kawabata K, Inamura M, Takayama K, Furukawa N, Sakurai F. Katayama K, Hayakawa H, Furue-Kusuda M, Mizuguchi H.	Adenovirus vector-mediated efficient transduction into human embryonic and induced pluripotent stem cells.	Cell. Reprogram.	12	501-507	2010
川端健二、田代克久、水口裕之.	iPS細胞への遺伝子導入を用いた分化誘導の最適化	薬学雑誌	130	1527-1534	2010

研究成果の刊行物・別刷

Gut Online First, published on January 20, 2012 as 10.1136/gutjnl-2011-300717

ORIGINAL ARTICLE

MicroRNA-221/222 upregulation indicates the activation of stellate cells and the progression of liver fibrosis

Tomohiro Ogawa,[1,2,3] Masaru Enomoto,[1] Hideki Fujii,[1] Yumiko Sekiya,[1,2] Katsutoshi Yoshizato,[2,4] Kazuo Ikeda,[5] Norifumi Kawada[1,2]

[1]Department of Hepatology, Graduate School of Medicine, Osaka City University, Osaka, Japan
[2]Liver Research Center, Graduate School of Medicine, Osaka City University, Osaka, Japan
[3]Center for the Advancement of Higher Education, Faculty of Engineering, Kinki University, Hiroshima, Japan
[4]PhoenixBio Co Ltd., Hiroshima, Japan
[5]Department of Anatomy and Cell Biology, Graduate School of Medicine, Nagoya City University, Aichi, Japan

Correspondence to
Professor Norifumi Kawada, Department of Hepatology, Graduate School of Medicine, Osaka City University, 1-4-3, Asahimachi, Abeno, Osaka 545-8585, Japan; kawadanori@med.osaka-cu.ac.jp

Revised 1 December 2011
Accepted 15 December 2011

ABSTRACT

Background MicroRNAs (miRNAs) are important in hepatic pathophysiology and the development of liver cancer.

Objective To explore miRNAs that are regulated with the progression of liver fibrosis caused by chronic liver disease.

Design The regulated miRNAs in human livers infected with hepatitis C virus were identified by microarray analysis. Their expression in human livers with non-alcoholic steatohepatitis, mouse livers from two fibrosis models and cultured stellate cells was validated by real-time RT-PCR. The regulation of miR-222 expression in stellate cells by nuclear factor kappa B (NF-κB) was assayed. Finally, the effects of an miR-222 precursor or inhibitor on the expression of cyclin-dependent kinase inhibitor 1B (CDKN1B) and the growth of LX-2 cells were determined.

Results It was found that miR-199a-5p/199a-3p and miR-221/222 were upregulated in the human liver in a fibrosis progression–dependent manner. Among these miRNAs, miR-221/222 were upregulated in LX-2 cells and increased during the course of culture-dependent activation of mouse primary stellate cells, in a manner similar to the expression of α1(I) collagen and α-smooth muscle actin mRNAs. The expression of miR-221/222 increased in mouse models of liver fibrosis. In contrast, an NF-κB inhibitor significantly suppressed the miR-222 induction that was stimulated in culture by transforming growth factor α or tumour necrosis factor α. Although overexpression or downregulation of miR-222 failed to regulate the growth of LX-2 cells, miR-222 bound to the *CDKN1B* 3′UTR and regulated the expression of the corresponding protein.

Conclusion miR-221/222 may be new markers for stellate cell activation and liver fibrosis progression.

Significance of this study

What is already known about this subject?
- The abundance of miR-221/222 increases in human hepatocellular carcinoma (HCC).
- miR-221/222 elicit their oncogenic effects via the downregulation of tumour suppressors, such as p27, p57 and PTEN.
- The expression of miR-221/222 is induced by NF-κB activation in prostate carcinoma and glioblastoma cells.

What are the new findings?
- The expression of miR-221/222 increases with the progression of human liver fibrosis and is correlated with the expression levels of α1 (I) collagen and α-smooth muscle actin mRNAs.
- The expression of miR-221/222 is highly correlated with α1 (I) collagen mRNA expression in mouse stellate cells in culture.
- miR-222 expression is inhibited by an NF-κB inhibitor and upregulated by NF-κB activators, such as tumour necrosis factor α and transforming growth factor α.

How might they impact on clinical practice in the foreseeable future?
- miR-221/222 have the potential to be new markers for stellate cell activation and liver fibrosis progression in humans.
- The pattern of miR-221/222 expression can serve as a useful tool for understanding and investigating the mechanism of the progression of liver fibrosis.
- The miRNA profiling of human liver fibrosis contributes to the identification of predictors of disease prognosis and potential therapeutic targets.

INTRODUCTION

Hepatic fibrosis is a consequence of the accumulation of extracellular matrix (ECM) components in the liver. This process is caused by the persistent liver damage and wound healing reaction induced by chronic viral hepatitis, alcohol abuse, non-alcoholic steatohepatitis (NASH) and several other aetiologies and can progress to cirrhosis and hepatocellular carcinoma (HCC).[1] Hepatitis C virus (HCV) infection is one of the leading causes of end-stage liver diseases worldwide and the most common indication for liver transplantation in the USA and Europe. In addition, non-alcoholic fatty liver disease and its progressive form, NASH, have become urgent clinical problems owing to the increasing prevalence of metabolic syndrome.[2–4] Because fibrotic liver disease has thus become a global health problem, it is important to understand the molecular mechanisms of hepatic fibrosis, irrespective of the cause, to establish proper therapeutic strategies and to identify diagnostic markers of this disease.

It is generally accepted that excessive production of ECM components by activated hepatic stellate cells and myofibroblasts is responsible for hepatic fibrosis.[5 6] Hepatic stellate cells exist in Disse's space and store vitamin A under physiological conditions.[7] When liver injury occurs, these cells become activated in response to oxidative stress, growth factors and inflammatory stimuli that are produced by damaged hepatocytes, resident macrophages (Kupffer cells), infiltrating inflammatory cells and aggregated platelets. The hepatic stellate cells then undergo transformation into myofibroblast-like cells that express α-smooth muscle actin (αSMA).[5] Activated stellate cells deposit ECM components, including types I and III collagen, fibronectin and laminin, at the site of local tissue damage and secrete profibrogenic mediators, such as transforming growth factor β (TGFβ), connective tissue growth factor and platelet-derived growth factor, thereby playing a pivotal role in liver fibrogenesis.[6]

MicroRNAs (miRNAs) are small, endogenous, non-coding RNAs that interact with the 3′ untranslated region (UTR) of target mRNAs, resulting in the inhibition of translation or the promotion of mRNA degradation.[8 9] miRNAs are important in proliferation,[10] development[11] and differentiation[12] in many cell types and are involved in the development of many diseases, including cancer.[13–15] miR-122 has been the best studied miRNA with regard to liver pathophysiology. For example, miR-122 is highly abundant in the human liver and is essential for HCV replication.[16–19] Interferon β rapidly modulates the expression of miR-122, which has sequence-predicted targets within the HCV RNA.[20] In chronic hepatitis C, decreased miR-122 has been associated with an absence of virological response to interferon and ribavirin treatment.[21] miR-21, -34a, -93, -96, -221/222 and -519a increase and, in contrast, let-7c decreases in human HCC.[22] The expression levels of miR-21 and miR-122 correlate with the histological evaluation of HCV-induced liver disease.[23]

Here, we show that the expression of miR-221/222 increased with the progression of liver fibrosis and significantly correlated with the expression of α1 (I) collagen (Col1A1) and αSMA mRNAs in human fibrotic livers. The expression of miR-221/222 in human fibrotic livers was also reproduced in mouse models of hepatic fibrosis. Interestingly, miR-221/222 were more highly expressed in a human stellate cell line, LX-2, than in HCC cell lines and their expression was induced with the activation of mouse stellate cells. Finally, we show that the expression of miR-222 in stellate cells may be regulated by the activation of nuclear factor kappa B (NF-κB). Taken together, our findings indicate that miR-221/222 upregulation is a new marker for stellate cell activation and liver fibrosis progression that could be used for the clinical diagnosis of liver fibrosis.

MATERIALS AND METHODS

Materials

Precursors and inhibitors of miR-222 and the negative control miRNA were purchased from Ambion (Austin, Texas, USA). Dulbecco's modified Eagle's medium (DMEM) and fetal bovine serum (FBS) were purchased from Sigma Chemical Co (St Louis, Missouri, USA). The mouse monoclonal antibody against cyclin-dependent kinase inhibitor 1B (CDKN1B (p27, Kip1)) was from Cell Signaling Technology Inc (Beverly, Massachusetts, USA) and that against glyceraldehyde 3-phosphate dehydrogenase (GAPDH) was from Chemicon International Inc (Temecula, California, USA). Enhanced Chemiluminescence Plus detection reagent was from GE Healthcare (Buckinghamshire, UK). Immobilon P membranes were from Millipore Corp. (Bedford, Massachusetts, USA). Recombinant human TGFα and mouse tumour necrosis factor (TNF)α were from R&D Systems, Inc (Minneapolis, Minnesota, USA). 6-Amino-4-(4-phenoxyphenylethylamono)quinazoline (QNZ) was from EMD Chemicals, Inc (Gibbstown, New Jersey, USA). All other reagents were purchased from Sigma Chemical Co or Wako Pure Chemical Co (Osaka, Japan).

Liver biopsy specimens

Liver biopsy specimens were obtained from 35 patients with chronic hepatitis C genotype 1 infection and 26 patients with NASH using a 15-gauge Tru-Cut biopsy needle (Hakko Inc., Tokyo, Japan) under ultrasound guidance (table 1). Of the 26 patients with NASH, oral hypoglycaemic agents were given to four patients (sulphonylureas to three and metformin to one), antihypertensive agents to eight (angiotensin receptor blockers to five and calcium channel blockers to three) and antihyperlipidaemic agents to eight (statins to five and fibrates to three) at the time of liver biopsy. Informed consent was obtained from all patients before biopsy. All procedures were in accordance with the Helsinki Declaration of 1975 (2008 revision). Biopsied liver tissues were fixed in 10% formalin solution and then embedded in paraffin. The stage of liver fibrosis was evaluated according to the METAVIR scoring system in patients with chronic hepatitis C[24] and the Brunt classification in patients with NASH.[4] A portion of each biopsy sample was immediately placed in RNAlater (Qiagen, Valencia, California, USA), temporarily stored at −20°C and then used to extract total RNAs using the mirVana miRNA Isolation Kit (Applied

Table 1 Baseline characteristics of patients

Characteristics	All patients with CHC (n=35)	Patients with CHC undergoing microarray analysis (n=22)	Patients with NASH (n=26)
Age (years)*	59±9	58±6	58±12
Female sex (%)†	20 (57)	11 (50)	14 (54)
Interferon-naïve (%)†	24 (69)	15 (68)	
ALT (IU/l)‡	57 (34–99)	88 (51–171)	69 (28–226)
Albumin (g/dl)*	4.0±0.3	4.0±0.3	4.0±0.5
Platelet count ($\times 10^9$/l)*	179±53	169±46	184±54
HCV RNA ($\log_{10}$ copies/ml)*	6.1±1.0	6.0±1.2	
Grade of necroinflammation† (A0/A1/A2/A3)	3/23/8/1	2/13/6/1	0/10/10/6
Stage of fibrosis† (F1/F2/F3/F4)	19/7/7/2	11/4/5/2	7/8/8/3

*Mean±SD.
†Numbers of patients.
‡Median (IQR).
ALT, alanine aminotransferase; CHC, chronic hepatitis C; HCV, hepatitis C virus; NASH, non-alcoholic steatohepatitis.

Biosystems, Foster City, California, USA). As controls, normal liver tissues were taken from four patients who underwent resection for metastatic liver tumours.

Microarray analysis

In 22 of the 35 patients with chronic hepatitis C and in four controls, microarray analysis was performed using 10 μg total RNA with the 3D-Gene Human miRNA Oligo chip v10.1 (Toray, Tokyo, Japan), as described in detail elsewhere.[25]

Mouse model of liver fibrosis

Male C57BL/6 mice, 7–10 weeks old, were purchased from Japan SLC, Inc (Shizuoka, Japan). All animals received humane care. The experimental protocol was approved by the Committee of Laboratory Animals according to institutional guidelines. Mice (n=5) were injected intraperitoneally with 200 μg/g body weight of thioacetamide (TAA, Sigma) diluted in saline three times a week for 4 or 8 weeks.[26] Control mice (n=5) were injected with saline. As another liver fibrosis model, mice were given either a methionine- and choline-deficient diet (MCDD, n=7) or methionine-choline control diet (MCCD, n=7) for 5 or 15 weeks, as previously described.[27] In addition, a similar model was generated in rats by giving them MCCD for 10 weeks, MCDD for 10 weeks, or MCDD for 8 weeks followed by MCCD for the last 2 weeks (recovery group).[27] The ingredients for these diets were purchased from MP Biomedicals (Solon, Ohio, USA).

Cells

Primary stellate cells were isolated from male C57BL/6 mice by the pronase-collagenase digestion method[28] and were cultured in DMEM supplemented with 10% FBS. Hepatocytes were isolated by collagenase digestion. One day after culturing, the cells were treated with TGFα (1–10 ng/ml), TNFα (0.1–1 ng/ml), or QNZ (10–100 nmol/l) for 24 or 72 h. LX-2 (donated by Dr Scott Friedman[29]), NIH3T3 and Huh7 cells were maintained on plastic culture plates in DMEM supplemented with 10% FBS. HepG2 cells (JCRB1054), obtained from the Health Science Research Resources Bank (Osaka, Japan), were maintained on plastic culture plates in Minimum Essential Medium (Invitrogen, Carlsbad, California, USA) supplemented with 10% FBS, 1 mM sodium pyruvate (Invitrogen) and 1% non-essential amino acids (Invitrogen).

Quantitative real-time PCR

Total RNA was extracted from cells and liver tissues using the miRNeasy Mini Kit (Qiagen). cDNAs were synthesised using 0.5 μg of total RNA, a ReverTra Ace qPCR RT Kit (Toyobo, Osaka, Japan) and oligo(dT)$_{12-18}$ primers, according to the manufacturer's instructions. Gene expression was measured by real-time PCR using the cDNAs, THUNDERBIRD SYBR qPCR Mix Reagents (Toyobo) and gene-specific oligonucleotide primers (listed in table 2) with an ABI Prism 7500 Real-Time PCR System (Applied Biosystems). The GAPDH level was used to normalise the relative abundance of mRNAs. To detect miRNA expression, the RT reaction was performed using the TaqMan MicroRNA Assay (Applied Biosystems). Primers for PCR reactions in the miRNA assays were obtained from Applied Biosystems.

Immunoblotting

Proteins (20 μg) were subjected to sodium dodecyl sulphate–polyacrylamide gel electrophoresis and then transferred onto Immobilon P membranes. After blocking, the membranes were treated with primary antibodies followed by peroxidase-conjugated secondary antibodies. Immunoreactive bands were visualised by the enhanced chemiluminescence system using the Fujifilm Image Reader LAS-3000 (Fuji Medical Systems, Stamford, Connecticut, USA).

Table 2 List of primer sequences

Gene		Sequence (5′-3′)	Accession No
Human	Forward	CCCGGGTTTCAGAGACAACTTC	NM_000088
Col1A1	Reverse	TCCACATGCTTTATTCCAGCAATC	
Human	Forward	GACAATGGCTCTGGGCTCTGTAA	NM_001613
αSMA	Reverse	CTGTGCTTCGTCACCCACGTA	
Human	Forward	AGCTTGCCCGAGTTCTACTACAG	NM_004064
CDKN1B	Reverse	ACCAAATGCGTGTCCTCAGAGT	
Human	Forward	CTCTACTGGCGAAACCTGTATCC	NM_000089
Col1A2	Reverse	TCTCCTAGCCAGACGTGTTTCTT	
Human	Forward	CTGGCCACAACTGCCAAATG	NM_001145938
MMP1	Reverse	CTGTCCCTGAACAGCCCAGTACTTA	
Human	Forward	TGACATCAAGGGCATTCAGGAG	NM_001127891
MMP2	Reverse	TCTGAGCGATGCCATCAAATACA	
Human	Forward	TCGAACTTTGACAGCGACAAGAA	NM_004994
MMP9	Reverse	TCAGTGAAGCGGTACATAGGGTACA	
Human	Forward	GGATACTTCCACAGGTCCCACAA	NM_003254
TIMP1	Reverse	CTGCAGGTAGTGATGTGCAAGAGTC	
Human	Forward	GGAGCACTGTGTTTATGCTGGAA	NM_003255
TIMP2	Reverse	GACCGAGCGATTGCTCAAGA	
Human	Forward	AGCGACTCGCCAGAGTGGTTA	NM_000660
TGFβ1	Reverse	GCAGTGTGTTATCCCTGCTGTCA	
Human	Forward	GCACCGTCAAGGCTGAGAAC	NM_002046
GAPDH	Reverse	TGGTGAAGACGCCAGTGGA	
Mouse	Forward	CCTGGCAAAGACGGACTCAAC	NM_007742
Col1A1	Reverse	GCTGAAGTCATAACCGCCACTG	
Mouse	Forward	TCCCTGGAGAAGAGCTACGAACT	NM_007392
αSMA	Reverse	AAGCGTTCGTTTCCAATGGT	
Mouse	Forward	TGCACCACCAACTGCTTAG	NM_008084
GAPDH	Reverse	GGATGCAGGGATGATGTTC	

Col1A1, α1 (I) collagen; GAPDH, glyceraldehyde 3-phosphate dehydrogenase; MMP, matrix metalloproteinase; αSMA, α-smooth muscle actin; TIMP, tissue inhibitor of matrix metalloproteinase.

Transient transfection with miRNA precursors and inhibitors

Precursors or inhibitors of miR-222 and the negative control miRNA were transfected into human and mouse stellate cells using Lipofectamine RNAiMAX Transfection Reagent (Invitrogen) at a final concentration of 50 nmol/l, as previously described.[30 31] After 6 h, the culture medium was changed. Then, after 24 h, the cells were collected for total RNA and protein extraction.

Luciferase reporter assay

The interaction of the *CDKN1B* 3′UTR with miR-222 was assayed basically according to a previously described method.[30 31] The *CDKN1B* 3′UTR was obtained by PCR using human stellate cell cDNA as a template and the primer set forward 5′-TTCTCGAGGTTCTTGTCTTGATGTGTCACC-3′, reverse 5′-TTTCTAGAGAGAGCAGAGGCCTGAGAAG-3′. The Dual-Glo Luciferase Assay System (Promega, Madison, Wisconsin, USA) was used to analyse luciferase expression, according to the manufacturer's protocol.

Cell proliferation assay

LX-2 cells were plated at a density of 3×10^3 cells/well in 96-well plates for 24 h and were then transfected with the miR-222 precursor or inhibitor as described above. After 24 h, the medium was changed and culturing was continued for an additional

1–3 days before measuring cell proliferation by the WST-1 assay.[31]

Statistical analysis

Data, presented as box plots, are the median, IQR, minimum and maximum. The Mann–Whitney U test was used to analyse the distribution of continuous variables. The Jonckheere–Terpstra test for ordered alternatives was used to identify trends among classes. Correlation coefficients between parameters were evaluated by Spearman rank correlations. A two-tailed p value <0.05 was considered significant.

RESULTS

Patient characteristics

Table 1 shows the baseline characteristics of the patients infected with HCV and those with NASH who were included in this study. There were no significant differences in clinical, biochemical, haematological, virological, or histological characteristics between the 22 patients with HCV who were analysed by microarray and the 13 patients with HCV who were not.

miRNA expression profile in patients with HCV

We comprehensively compared miRNA expression profiles between cases of mild liver fibrosis (F1/F2) and advanced liver fibrosis (F3/F4) among the 22 patients with HCV using microarray analysis. As shown in the heat map in figure 1, 18 miRNAs were significantly upregulated (fold change, 1.21 to 2.59), whereas six miRNAs were significantly downregulated (fold change, −1.69 to −1.20) in livers with advanced fibrosis. Among the 18 overexpressed miRNAs, p values of <0.01 were found for miR-222 (fold change, 1.80), miR-214 (fold change, 1.84), miR-199a-3p (miR-199b-3p) (fold change, 1.90) and miR-199a-5p (fold change, 2.00). Among the six downregulated miRNAs, miR-422a (fold change, −1.69) showed a p value <0.01. Among them, the abundance of miR-199a-5p and miR-199a-3p has previously been reported to be increased in fibrotic liver disease.[32]

Next, we quantitatively confirmed our miRNA expression results in 35 patients with HCV (table 1) using real-time PCR. miR-199a-5p, miR-199a-3p and miR-222 were significantly upregulated in a stepwise manner according to the progression of liver fibrosis (figure 2A). miR-222 forms a cluster with miR-221 in the human and mouse genomes. In fact, miR-221 expression was significantly upregulated in patients with HCV with severe fibrosis (figure 2A). Col1A1 mRNA expression also significantly increased with increasing progression of liver fibrosis (figure 2B) and was significantly correlated with the expression of miR-222 ($r=0.843$, $p<0.001$) (figure 2C). Additionally, αSMA mRNA expression tended to increase according to the progression of fibrosis (figure 2B) and was significantly correlated with the expression of miR-222 ($r=0.701$, $p<0.001$) (figure 2C).

MicroRNA-221/222 expression in patients with NASH

We also validated miR-221 and miR-222 expression in 26 patients with biopsy-proven NASH (F1, seven; F2, eight; F3, eight; F4, three) by real-time PCR. The expression of these miRNAs was significantly upregulated in a manner dependent on the progression of liver fibrosis (figure 3A). Col1A1 mRNA expression was also significantly upregulated (figure 3B) and correlated with the expression of miR-222 ($r=0.626$, $p<0.001$) (figure 3C). In contrast, the expression level of αSMA mRNA tended towards a correlation with that of miR-222, but this result was not significant ($r=0.375$, $p=0.059$) (figure 3B,C). These results indicate the close correlation between miR-222 and Col1A1 mRNA expression in human liver fibrosis caused by NASH.

Expression of miR-221/222 in rodent models of liver fibrosis

Next, we studied miR-221 and miR-222 expression in mouse models of liver fibrosis. First, liver fibrosis was induced in mice by injecting TAA for 8 weeks. As shown in figure 4A, haematoxylin and eosin staining and Sirius red staining confirmed the occurrence of liver fibrosis, in particular around the central vein

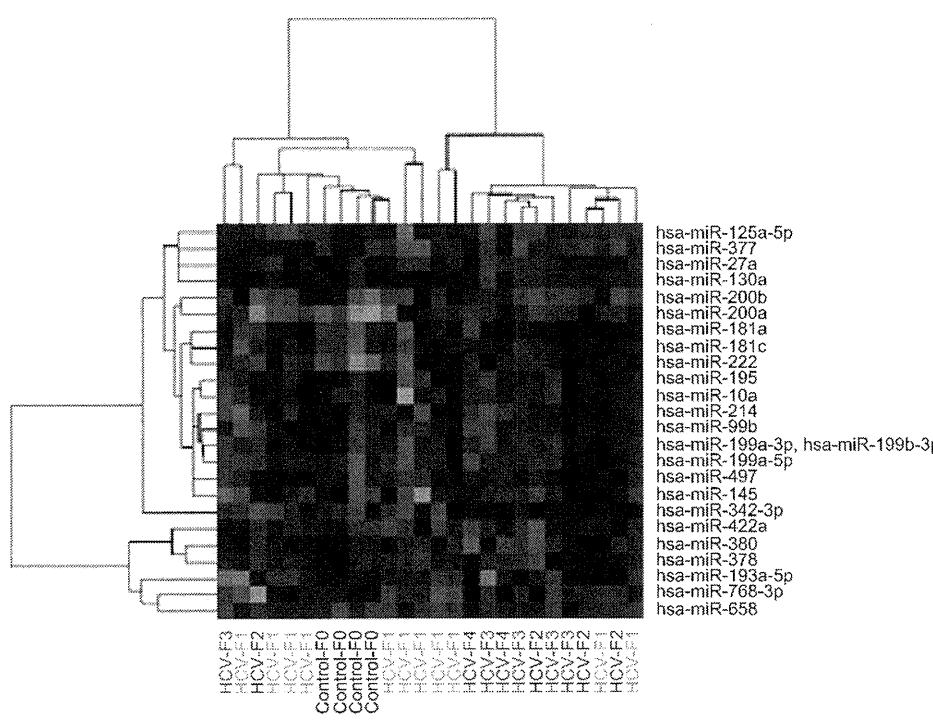

Figure 1 Heat map of microRNA (miRNA) expression in human liver tissue. Shown is the clustering of patients (n=22) with chronic hepatitis C by comprehensive analysis of intrahepatic miRNA expression according to the degree of hepatic fibrosis in biopsy specimens. Green and red denote downregulated and upregulated genes, respectively. F, fibrosis stage; HCV, hepatitis C virus.

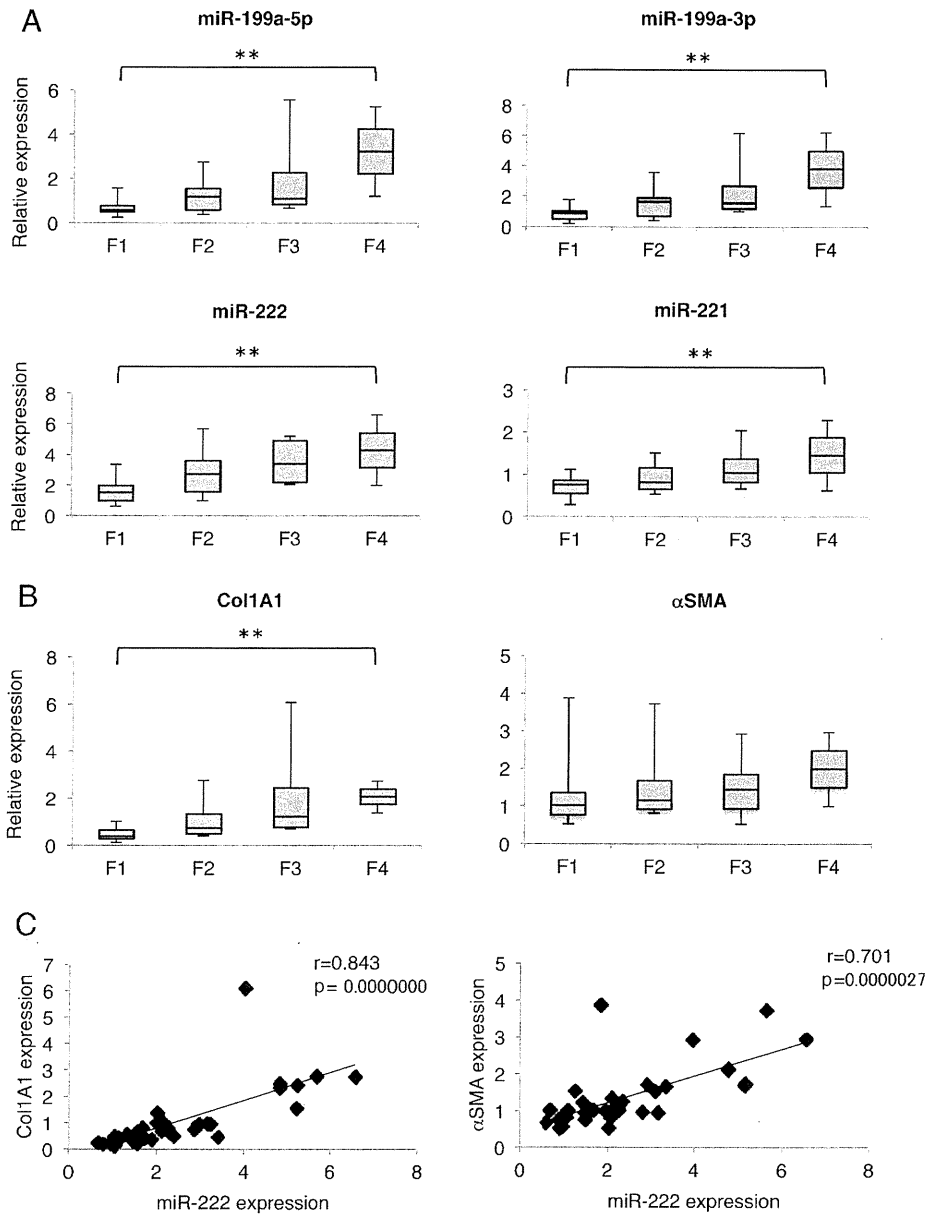

Figure 2 MicroRNA (miRNA) levels and their correlations with Col1A1 and α-smooth muscle actin (αSMA) mRNA expression in patients with chronic hepatitis C. (A) Expression of miR-199a-5p, miR-199a-3p, miR-222 and miR-221 in 35 patients with hepatitis C virus (HCV) with fibrosis. The expression levels are indicated relative to F1. The Jonckheere–Terpstra test for ordered alternatives was used to identify trends among classes. **p<0.01. (B) Expression of Col1A1 and αSMA mRNAs in 35 patients with HCV with fibrosis. The expression levels are indicated relative to F1. Glyceraldehyde 3-phosphate dehydrogenase was used as an internal control. The Jonckheere–Terpstra test for ordered alternatives was used to identify trends among classes. **p<0.01. (C) Correlation between miR-222 expression and Col1A1 or αSMA mRNA expression. Correlation coefficients between parameters were evaluated by Spearman rank correlations.

area. These mouse livers exhibited significant upregulation of the expression of Col1A1 (3.1-fold, p<0.05) and αSMA (1.9-fold, p<0.05) mRNAs compared with the control livers at 8 weeks (figure 4B). The expression of miR-221 and miR-222 increased by 1.8-fold (p=0.06) and 1.4-fold (p<0.01), respectively, at 8 weeks after TAA injection (figure 4C). The increased expression of miR-222 was accompanied by increased Col1A1 (p<0.05) and αSMA mRNA expression (p<0.01) (data not shown). Another liver fibrosis model was produced in mice by feeding them an MCDD. miR-221 and miR-222 increased by 2.4-fold (p<0.01) and 2.6-fold (p<0.01), respectively, in livers of mice fed MCDD for 15 weeks compared with those fed MCCD for 15 weeks (figure 4D). These results confirm that the increased expression of miR-221/222 in fibrotic livers is reproduced in mouse models. In addition, miR-221 and miR-222 expression increased in rats administered MCDD for 10 weeks, but returned to the level of the controls after 2 weeks on MCCD in the recovery group (figure 4E). These data clearly indicate the correlation between the increase in miR-221/222 and liver fibrosis.

Expression of miR-222 in hepatic stellate cells

According to the data obtained from human and rodent fibrotic livers, we assumed that stellate cells may contribute to the increases of miR-222 and its homologue miR-221. As expected, the expression of both miR-221 and miR-222 increased during the activation process of mouse stellate cells in primary culture (6.1- and 26.8-fold increases in miR-221 and 4.1- and 13.9-fold increases in miR-222 at day 4 and day 7 compared with day 1, respectively), in a manner similar to the mRNA expression of Col1A1 and αSMA (38.3- and 61.3-fold increases in Col1A1 mRNA and 6.1- and 6.9-fold increases in αSMA at day 4 and day 7 compared with day 1, respectively) (figure 5A,B). Isolated mouse hepatocytes expressed both miRNAs in smaller amounts than with the activated stellate cells (figure 5A). In addition, both miR-221 and miR-222 expression were significantly higher in LX-2 than in HepG2 cells (9.5- and 6.0-fold, respectively), Huh7 cells (9.2- and 4.4-fold, respectively) and NIH3T3 cells (1.1- and 3.2-fold, respectively) (figure 5C), confirming the relative specificity of the miRNA expression in activated stellate cells.

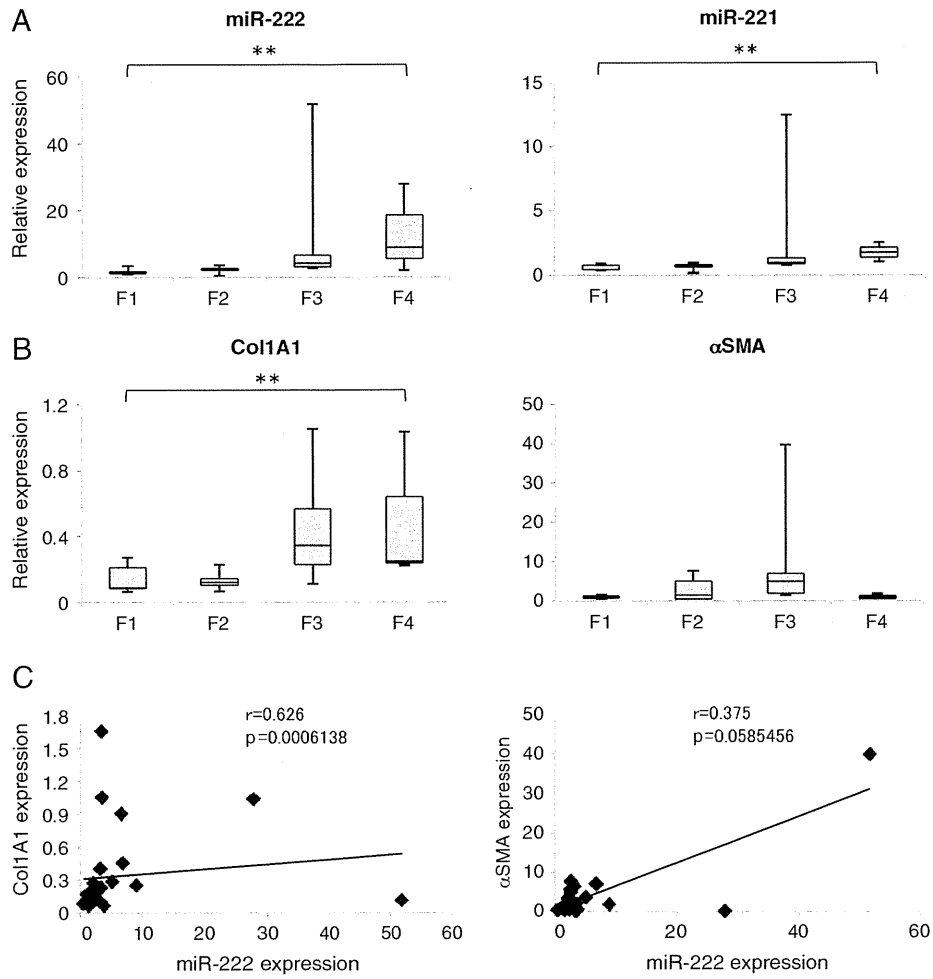

Figure 3 Levels of microRNA (miRNA)-221/222 and their correlation with Col1A1 and α-smooth muscle actin (αSMA) mRNA levels in patients with non-alcoholic steatohepatitis (NASH). (A) Expression of miR-221/222 in 26 patients with NASH. The expression levels are indicated relative to F1. The Jonckheere–Terpstra test for ordered alternatives was used to identify trends among classes. **p<0.01. (B) Expression of Col1A1 and αSMA mRNAs in 26 patients with NASH. The expression levels are indicated relative to F1. Glyceraldehyde 3-phosphate dehydrogenase was used as an internal control. The Jonckheere–Terpstra test for ordered alternatives was used to identify trends among classes. **p<0.01. (C) Correlation between miR-222 expression and Col1A1 or αSMA mRNA expression. Correlation coefficients between parameters were evaluated by Spearman rank correlations.

miR-222 transcription is regulated by NF-κB; the genomic region upstream of human miR-222 has multiple NF-κB binding elements.[33] NF-κB regulates Col1A1 gene expression and stellate cell activation.[34–36] Thus, we studied whether NF-κB stimulators, such as TGFα and TNFα, induce miR-222 expression and, in contrast, whether an NF-κB inhibitor (QNZ) inhibits its expression. As shown in figure 5D, stimulation of stellate cells with TGFα (1 or 10 ng/ml) or TNFα (0.1 or 1 ng/ml) for 24 h from day 1 to day 2 upregulated miR-222 expression, while QNZ (10 or 100 nmol/l) significantly reduced it. Stimulation of stellate cells with TGFα (1 ng/ml) or TNFα (0.1 ng/ml) for 72 h from day 1 to day 4 upregulated miR-222 expression by 1.9-fold (p<0.01) or 1.3-fold (p<0.05), respectively, compared with the untreated control (figure 5E) and miR-222 upregulation was inhibited to 18% or 26% of the untreated control level, respectively, by QNZ (figure 5E). These results indicate that miR-222 expression in stellate cells is regulated by NF-κB activation. QNZ (10 nmol/l) inhibited the activation-associated morphological transition of mouse hepatic stellate cells (figure 5F). This condition attenuated the expression of Col1A1 mRNA to 21% (p<0.01) and αSMA mRNA to 63% (p<0.01) of the untreated control levels (figure 5G).

Interaction of miR-222 with the *CDKN1B* 3′UTR in human stellate cells

miR-221 controls CDKN1B and CDKN1C expression in HCC cell lines.[37] The prediction of miRNA target regions by TargetScan (http://www.targetscan.org/) indicated that the *CDKN1B* 3′UTR has two target regions for miR-221/222 (figure 6A). Here, we investigated the presence of a direct interaction between miR-222 and CDKN1B mRNA in LX-2 cells by the firefly luciferase reporter assay and found that the miR-222 precursors inhibited luciferase activity derived from vectors carrying the *CDKN1B* 3′UTR (figure 6B). These observations indicate that the *CDKN1B* 3′UTR could be targeted by miR-222 in LX-2 cells.

Next, we transfected miR-222 precursors and miR-222 inhibitors into LX-2 cells. The transient transfection of miR-222 precursors significantly inhibited CDKN1B mRNA and protein expression compared with their expression in cells transfected with the negative control miRNA (figure 6C). Additionally, the transfection of miR-222 inhibitors significantly upregulated CDKN1B mRNA and protein expression in comparison with cells transfected with the negative control miRNA (figure 6D). Even though the transfection of miR-222 precursors or inhibitors into LX-2 cells showed negligible effects on cell growth (figure 6E,F), these results indicate that miR-222 targets *CDKN1B* in LX-2 cells.

Additional analyses indicated that transient transfection with miR-222 precursors significantly upregulated Col1A1 and matrix metalloproteinase 2 (MMP-2) mRNA expression and downregulated MMP-1, MMP-9 and TGFβ1 mRNA expression via unknown mechanisms (figure 6G).

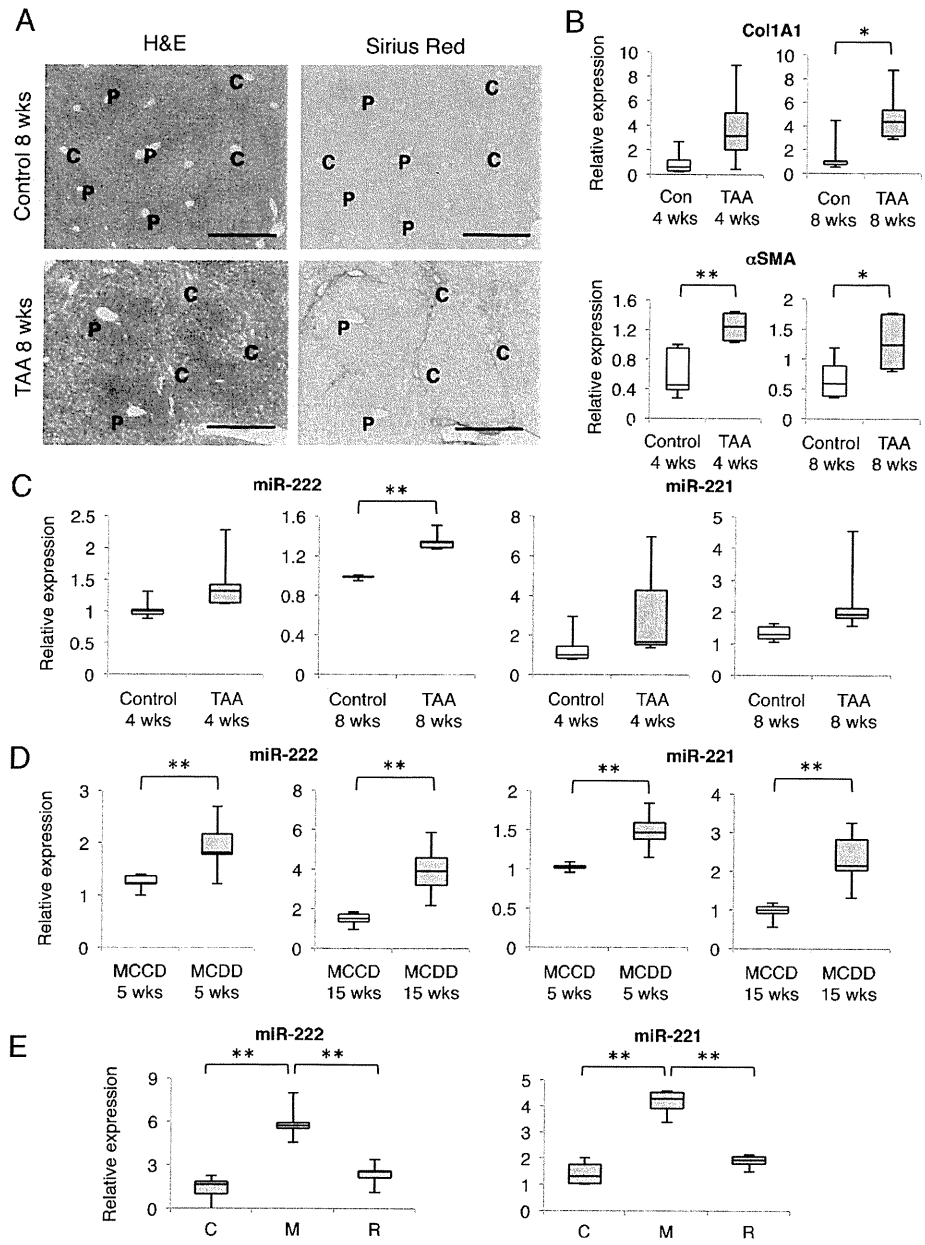

Figure 4 Expression of miR-221/222 in mouse models of liver fibrosis. (A) Liver fibrosis was induced in mice by injecting 200 μg/g body weight of thioacetamide (TAA) for 8 weeks. Haematoxylin and eosin staining (H&E; left). Sirius red staining (right). Scale bars, 200 μm. C, central vein area; P, portal vein area. (B) mRNA expression of Col1A1 and α-smooth muscle actin (αSMA) in TAA-induced liver fibrosis. The expression levels are indicated relative to control livers. Glyceraldehyde 3-phosphate dehydrogenase was used as an internal control. *$p<0.05$, **$p<0.01$ compared with control. (C) Expression of miR-221 and miR-222 in TAA-induced liver fibrosis. The expression levels are indicated relative to control livers. **$p<0.01$ compared with control. In B and C, open columns indicate data from controls and closed columns from TAA. (D) Expression of miR-221 and miR-222 in a methionine- and choline-deficient diet (MCDD)-induced liver fibrosis. The expression levels are indicated relative to methionine-choline control diet (MCCD) mouse livers. **$p<0.01$ compared with MCCD. Open columns indicate data from MCCD and closed columns from MCDD. (E) Expression of miR-221 and miR-222 in MCDD-induced liver fibrosis in rats.[27] The expression levels are indicated relative to rats fed MCCD for 10 weeks (C). Liver miR-221 and miR-222 levels significantly decreased in the recovery phase (R, MCDD for 8 weeks followed by MCCD for 2 weeks) compared with those fed MCDD for 10 weeks (M). **$p<0.01$.

DISCUSSION

Our study explored miRNA expression profiles during the progression of liver fibrosis in patients infected with HCV using microarray analysis. The expression of miR-222 was significantly correlated with that of Col1A1 and αSMA mRNAs in patients with HCV and with the expression of miR-221. To our knowledge, this is the first report to identify miR-221 and miR-221 as fibrosis-related molecules and to report miR-221/222 expression in a liver pathology other than carcinogenesis. Our results additionally indicate the close correlation between miR-221/222 and Col1A1 mRNA expression in the livers of people with NASH.

Recently, Roderburg *et al* reported the upregulation of miR-125-5p, miR-199b-3p, miR-221 and miR-302 and the downregulation of miR-29 family members in CCl_4-treated mouse livers, as observed using microarray analysis and quantitative RT-PCR.[38] Murakami *et al* reported that increased miR-199a-5p, miR-199a-3p, miR-200a and miR-200b levels are significantly associated with the progression of liver fibrosis in both humans and mice and that the overexpression of miR-199a-3p in human stellate cells results in the significant induction of tissue inhibitor of MMP-1, Col1A1 and MMP-13.[32] Furthermore, the expression levels of miR-21 and miR-122 have been correlated with the histological findings of HCV-induced liver disease.[23] However, in our analyses, although the expression of miR-199a-5p, miR-199a-3p and miR-21 tended to increase in activated mouse stellate cells during culture (0.8- and 2.1-fold for miR-199a-5p, 0.7- and 1.5-fold for miR-199a-3p and 1.9- and 3.8-fold for miR-21 at day 4 and day 7, respectively, compared with day 1), they failed to increase more than 10-fold, as miR-221 and miR-222 did (data not shown). Thus, miR-222 and miR-221 are more likely to reflect the activation of stellate cells than miR-199a-5p, miR-199a-3p and miR-21, similarly to the expression of Col1A1 mRNA.

It is generally accepted that liver fibrosis is a major risk factor for the development of HCC. A national surveillance

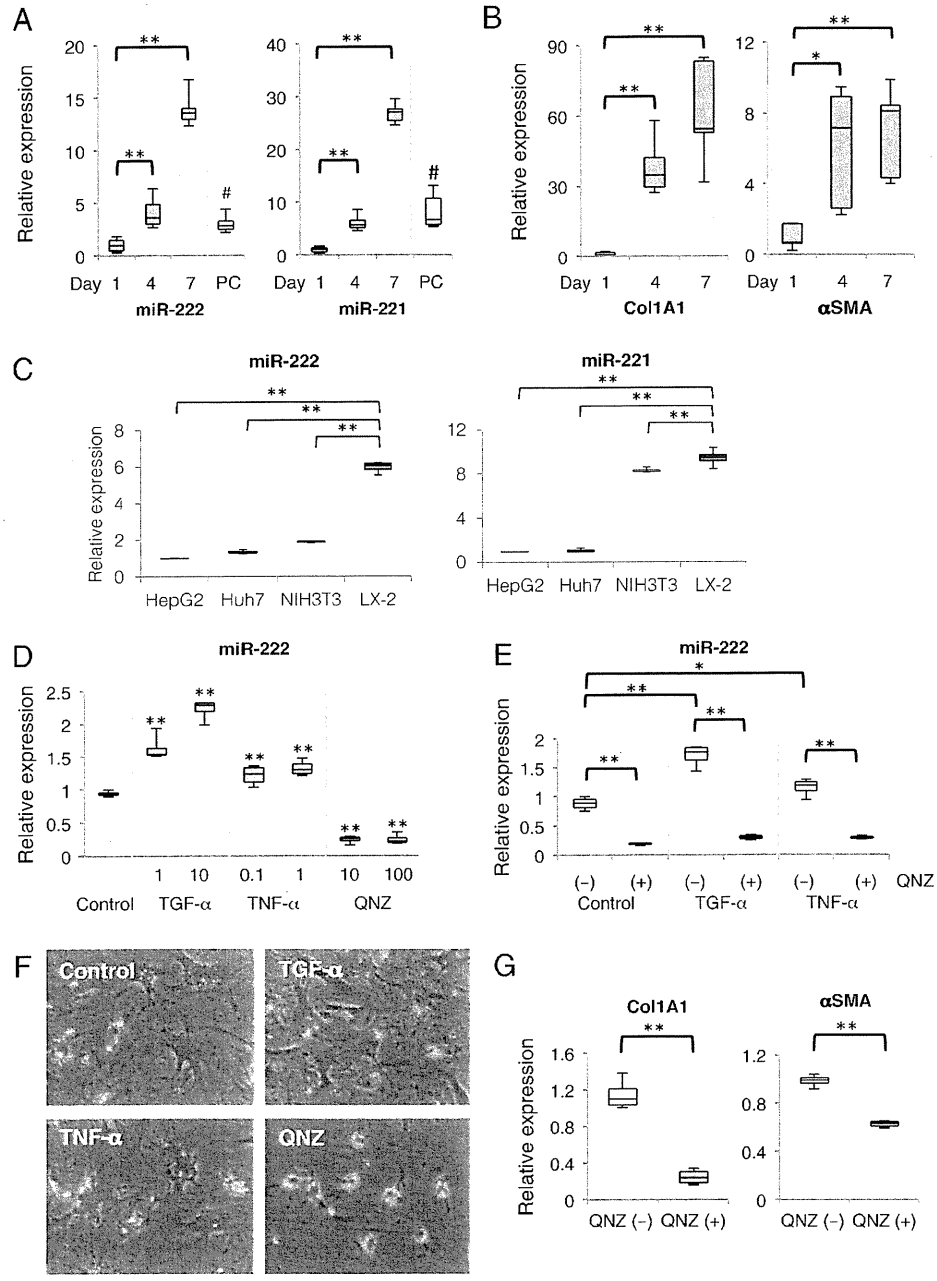

Figure 5 Regulation of miR-222 expression in stellate cells. (A) Expression of miR-221 and miR-222 in mouse stellate cells during primary culture. Isolated mouse stellate cells were cultured for the indicated periods. **p<0.01. PC indicates the expression of miR-221 and miR-222 in isolated mouse hepatocytes. #p<0.01 compared with stellate cells at day 7. (B) Expression of Col1A1 and α-smooth muscle actin (αSMA) mRNAs in mouse stellate cells during primary culture. Glyceraldehyde 3-phosphate dehydrogenase was used as an internal control. *p<0.05, **p<0.01. (C) Expression of miR-221 and miR-221 in HepG2, Huh7, NIH3T3 and LX-2. **p<0.01. (D and E) Regulation of miR-222 expression in mouse primary stellate cells. D: At 1 day after culture, the cells were treated with transforming growth factor α (TGFα; 1 or 10 ng/ml), tumour necrosis factor α (TNFα; 0.1 or 1 ng/ml), or 6-amino-4-(4-phenoxyphenylethylamono) quinazoline (QNZ; 10 or 100 nmol/l) for 24 h. Control indicates non-treated cells. **p<0.01 compared with control. E: At 1 day after culture, the cells were treated with TGFα (1 ng/ml), TNFα (0.1 ng/ml), QNZ (10 nmol/l), TGFα (1 ng/ml) plus QNZ (10 nmol/l), or TNFα (0.1 ng/ml) plus QNZ (10 nmol/l) for 72 h. Control indicates non-treated cells. *p<0.05, **p<0.01. (F) Morphology of mouse stellate cells observed under a microscope (×200) as in (E). (G) Expression of Col1A1 and αSMA mRNAs in mouse stellate cells treated with or without QNZ (10 nmol/l) during primary culture for 72 h.

programme in Japan has estimated that the annual incidence of HCC is 0.5–2.0% (mild liver fibrosis; F1/F2) and 5.3–7.9% (advanced liver fibrosis; (F3/F4) among patients with chronic hepatitis C.[39] miR-221 and miR-222, a pair of miRNAs encoded in a cluster on chromosome X, are overexpressed in a variety of human cancers, including HCC, in which they play oncogenic roles by downregulating p27, p57 and PTEN expression.[22 37 40] In particular, the pro-tumour activity of miR-221/222 is thought to be achieved by its regulation of CDKN1B (p27, Kip1).[41 42] In this study, we showed that miR-222 interacts with the *CDKN1B* 3′UTR and inhibits the expression of CDKN1B mRNA and protein in LX-2 cells, although it is unclear why increased miR-222 fails to affect the proliferation of stellate cells (figure 6). Type I interferon inhibits the proliferation of LX-2 cells by decreasing cyclin E and increasing p21 without affecting the expression of CDKN1B (p27).[31] In this regard, the proliferation of stellate cells may be strongly regulated by p21 rather than p27.

In general, miRNAs are transcribed by RNA polymerase II as part of capped and polyadenylated primary transcripts. The primary transcript is cleaved by the Drosha ribonuclease III to generate an approximately 70-nt stem-loop precursor miRNA, which is further cleaved by the cytoplasmic Dicer ribonuclease to generate the mature miRNA. In addition to this common pathway, recent investigations have shown that other factors are involved in the transcription of miRNAs by binding to their promoter regions. For instance, Galardi *et al* identified two separate regions upstream of the miR-221/222 promoter that are bound by the NF-κB subunit p65 and drive efficient transcription in luciferase reporter assays, indicating that the expression of miR-221/222 is induced by NF-κB activation in prostate carcinoma and glioblastoma cells.[33] Because NF-κB is involved in

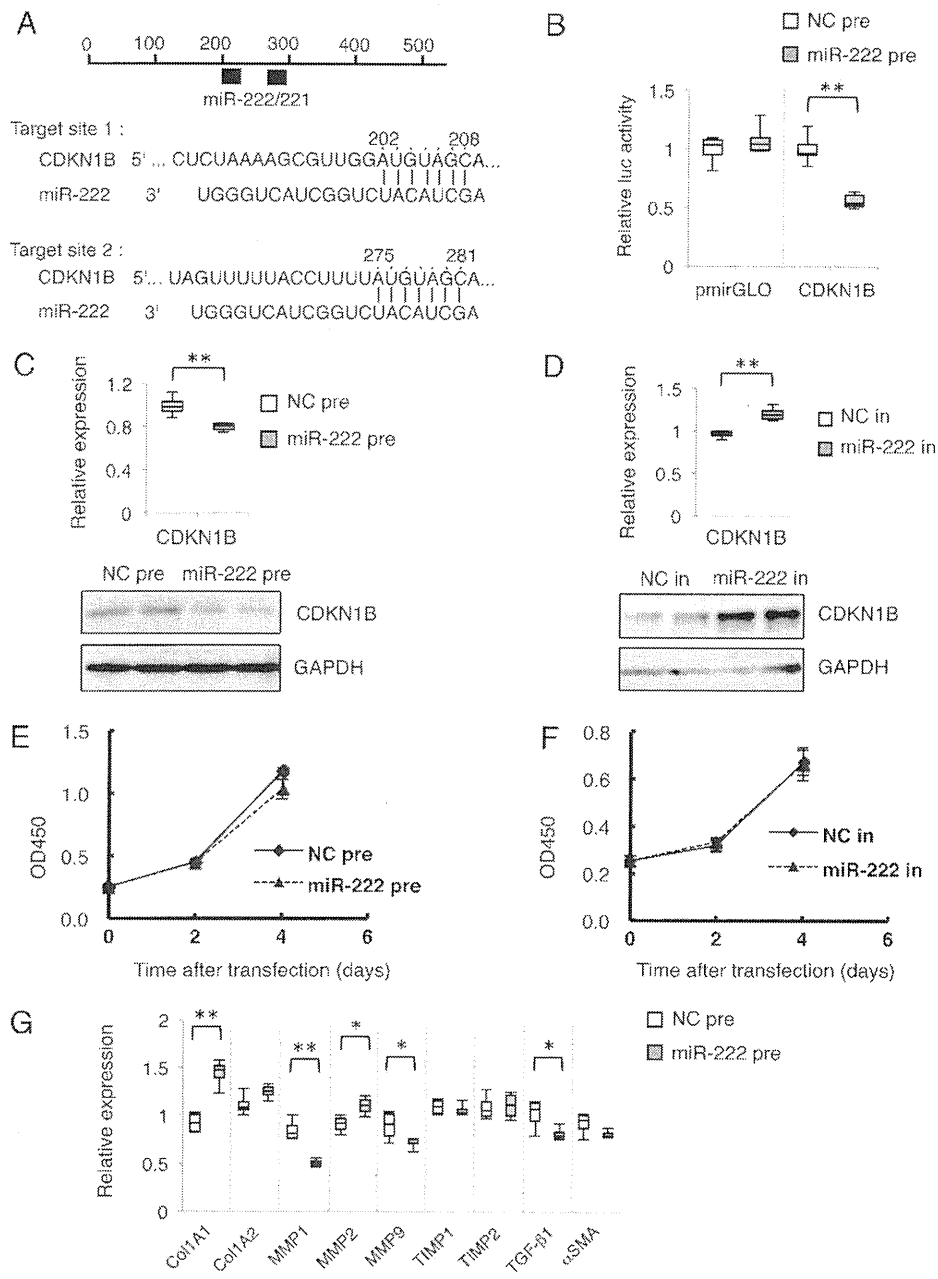

Figure 6 Interaction of miR-222 with the 3′UTR of CDKN1B mRNA. (A) Schematic indication of the miR-221/222 binding sites in the 3′UTR of CDKN1B mRNA based on TargetScan Human Release 5.1 (http://www.targetscan.org/). Black boxes indicate miR-221 or miR-222. Two predicted target sites of miR-221/222 are present in the 3′UTR of CDKN1B mRNA. (B) Reporter gene assay to test the interaction between the 3′UTR of CDKN1B mRNA and miR-222 in LX-2 cells. Relative luciferase activity derived from pCDKN1B—miR-222/mirGLO in the presence of miR-222 precursors. The pmirGLO vector was used as a negative control reporter vector. NC pre: co-transfection of reporter vectors together with a negative control miRNA precursor, which has a scrambled sequence. miR-222 pre: co-transfection of reporter vectors together with miR-222 precursors. The results are expressed relative to the activity in the presence of negative control precursors. **p<0.01. (C) Effect of miR-222 precursors on the expression of CDKN1B mRNA and protein in LX-2 cells. LX-2 cells were transfected with 50 nM miR-222 precursor (grey column) or a negative control (white column). At 24 h after transfection, CDKN1B mRNA (upper) and protein (lower) were measured. Glyceraldehyde 3-phosphate dehydrogenase (GAPDH) was used as an internal control. **p<0.01. (D) Effect of miR-222 inhibitors on the expression of CDKN1B mRNA and protein in LX-2 cells. LX-2 cells were transfected with 50 nM miR-222 inhibitor (grey column) or a negative control (white column). At 24 h after transfection, CDKN1B mRNA (upper) and protein (lower) were measured. GAPDH was used as an internal control. **p<0.01. (E, F) Effect of 50 nM miR-222 precursors (E) and inhibitors (F) on LX-2 cell growth, determined by WST-1 assay. (G) Effect of miR-222 precursors on the expression of fibrosis-related mRNAs in LX-2 cells. LX-2 cells were transfected with 50 nM miR-222 precursor (grey column) or a negative control (white column). At 24 h after transfection, the mRNAs were quantified. GAPDH was used as an internal control. *p<0.05, **p<0.01. ColA1, α1 (I) collagen; MMP, matrix metalloproteinase; αSMA, α-smooth muscle actin; TGFβ1, transforming growth factor β1; TIMP, tissue inhibitor of matrix metalloproteinase.

the process of stellate cell activation,[34–36] we speculated that the expression of miR-222 might be regulated through NF-κB activation in stellate cells. We found, however, that miR-222 expression was inhibited by QNZ, an NF-κB inhibitor, accompanied by the morphological maintenance of quiescence, and upregulated by the NF-κB activators TNFα and TGFα.

miRNA expression profiles can serve as useful tools for understanding and investigating the mechanism of the progression of liver fibrosis and can serve as new fibrosis biomarkers. miRNAs are packed into exosomes and circulate in blood.[43] However, this raises the question of whether circulating levels of miRNAs in blood correlate with the progression of liver fibrosis at the tissue level. Roderburg *et al* demonstrated that the expression levels of miR-29 family members in human liver fibrosis correlate with the downregulation of miR-29a in the serum.[38] Here, we observed that the expression of miR-222 in human livers with chronic trauma significantly correlated with the expression of Col1A1 mRNA, suggesting that miR-222 is a potential biomarker of liver fibrosis progression, although its utility as a serum biomarker needs further validation. Li *et al* recently reported that the miR-221 level in blood correlates with cirrhosis, tumour size and tumour stage and provides predictive value for prognosis in patients with HCC.[44]

This study has some limitations. The molecular mechanisms of liver fibrosis in viral hepatitis and in NASH may not exactly the same. In addition, fibrosis in human livers usually progresses

slowly, over the course of decades, so it is not practical to examine the expression of miRNAs at time points throughout progression. In contrast, liver fibrosis in experimental animals progresses quickly, so that within several weeks we could track the changes in miRNA expression at several time points. To establish the utility of miR-221/222 as biomarkers of liver fibrosis irrespective of aetiology, further studies are required to understand the exact mechanism by which the miRNAs participate in the progression of fibrosis.

In conclusion, we showed that miR-221 and miR-222 may be new markers for stellate cell activation and liver fibrosis progression in both humans and mice. These miRNAs could be used in the diagnosis of human liver fibrosis in clinical practice in the near future.

Acknowledgements We thank Drs Hiroyuki Motoyama, Le Thi Thanh Thuy, Masashi Iizuka and Tohru Komiya; Miss Shinobu Momen and Mrs Mami Mori for their valuable comments on this study.

Funding NK was supported by a grant-in-aid for scientific research from the Japan Society for the Promotion of Science (JSPS) (No 21390232; 2009—2011), a grant from the Ministry of Health, Labour and Welfare of Japan (2008—2010) and a Thrust Area Research Grant from Osaka City University (2008—2011). TO was supported by a grant-in-aid for scientific research from the JSPS (No 22790666; 2010—2011).

Competing interests None.

Ethics approval Ethics approval was provided by Osaka City University Medical School.

Contributors TO, EM, NK: conception, design, analysis and interpretation of data, drafting of the manuscript, critical revision of article, final approval given. HF, YS: analysis and interpretation of data, final approval given. KY, KI: conception, design, drafting of the manuscript, final approval given.

Provenance and peer review Not commissioned; externally peer reviewed.

REFERENCES

1. **Friedman SL.** Evolving challenges in hepatic fibrosis. *Nat Rev Gastroenterol Hepatol* 2010;**7**:425—36.
2. **Angulo P.** Nonalcoholic fatty liver disease. *N Engl J Med* 2002;**346**:1221—31.
3. **Matteoni CA,** Younossi ZM, Gramlich T, *et al.* Nonalcoholic fatty liver disease: a spectrum of clinical and pathological severity. *Gastroenterology* 1999;**116**:1413—19.
4. **Brunt EM,** Janney CG, Di Bisceglie AM, *et al.* Nonalcoholic steatohepatitis: a proposal for grading and staging the histological lesions. *Am J Gastroenterol* 1999;**94**:2467—74.
5. **Friedman SL.** Molecular regulation of hepatic fibrosis, an integrated cellular response to tissue injury. *J Biol Chem* 2000;**275**:2247—50.
6. **Kawada N.** Evolution of hepatic fibrosis research. *Hepatol Res* 2011;**41**:199—208.
7. **Wake K.** "Sternzellen" in the liver: perisinusoidal cells with special reference to storage of vitamin A. *Am J Anat* 1971;**132**:429—62.
8. **Filipowicz W,** Bhattacharyya SN, Sonenberg N. Mechanisms of post-transcriptional regulation by microRNAs: are the answers in sight? *Nat Rev Genet* 2008;**9**:102—14.
9. **Bartel DP.** MicroRNAs: genomics, biogenesis, mechanism and function. *Cell* 2004;**116**:281—97.
10. **Brennecke J,** Hipfner DR, Stark A, *et al.* bantam encodes a developmentally regulated microRNA that controls cell proliferation and regulates the proapoptotic gene hid in Drosophila. *Cell* 2003;**113**:25—36.
11. **Schratt GM,** Tuebing F, Nigh EA, *et al.* A brain-specific microRNA regulates dendritic spine development. *Nature* 2006;**439**:283—9.
12. **Chen CZ,** Li L, Lodish HF, *et al.* MicroRNAs modulate hematopoietic lineage differentiation. *Science* 2004;**303**:83—6.
13. **Kota J,** Chivukula RR, O'Donnell KA, *et al.* Therapeutic microRNA delivery suppresses tumorigenesis in a murine liver cancer model. *Cell* 2009;**137**:1005—17.
14. **Chen JF,** Murchison EP, Tang R, *et al.* Targeted deletion of Dicer in the heart leads to dilated cardiomyopathy and heart failure. *Proc Natl Acad Sci U S A* 2008;**105**:2111—16.
15. **Perkins DO,** Jeffries CD, Jarskog LF, *et al.* microRNA expression in the prefrontal cortex of individuals with schizophrenia and schizoaffective disorder. *Genome Biol* 2007;**8**:R27.
16. **Lewis AP,** Jopling CL. Regulation and biological function of the liver-specific miR-122. *Biochem Soc Trans* 2010;**38**:1553—7.
17. **Jopling CL,** Yi M, Lancaster AM, *et al.* Modulation of hepatitis C virus RNA abundance by a liver-specific MicroRNA. *Science* 2005;**309**:1577—81.
18. **Li YP,** Gottwein JM, Scheel TK, *et al.* MicroRNA-122 antagonism against hepatitis C virus genotypes 1-6 and reduced efficacy by host RNA insertion or mutations in the HCV 5' UTR. *Proc Natl Acad Sci U S A* 2011;**108**:4991—6.
19. **Lanford RE,** Hildebrandt-Eriksen ES, Petri A, *et al.* Therapeutic silencing of microRNA-122 in primates with chronic hepatitis C virus infection. *Science* 2010;**327**:198—201.
20. **Pedersen IM,** Cheng G, Wieland S, *et al.* Interferon modulation of cellular microRNAs as an antiviral mechanism. *Nature* 2007;**449**:919—22.
21. **Sarasin-Filipowicz M,** Krol J, Markiewicz I, *et al.* Decreased levels of microRNA miR-122 in individuals with hepatitis C responding poorly to interferon therapy. *Nat Med* 2009;**15**:31—3.
22. **Pineau P,** Volinia S, McJunkin K, *et al.* miR-221 overexpression contributes to liver tumorigenesis. *Proc Natl Acad Sci U S A* 2010;**107**:264—9.
23. **Marquez RT,** Bandyopadhyay S, Wendlandt EB, *et al.* Correlation between microRNA expression levels and clinical parameters associated with chronic hepatitis C viral infection in humans. *Lab Invest* 2010;**90**:1727—36.
24. **Bedossa P,** Poynard T. An algorithm for the grading of activity in chronic hepatitis C. The METAVIR Cooperative Study Group. *Hepatology* 1996;**24**:289—93.
25. **Sato F,** Tsuchiya S, Terasawa K, *et al.* Intra-platform repeatability and inter-platform comparability of microRNA microarray technology. *PLoS One* 2009;**4**:e5540.
26. **Ikejima K,** Honda H, Yoshikawa M, *et al.* Leptin augments inflammatory and profibrogenic responses in the murine liver induced by hepatotoxic chemicals. *Hepatology* 2001;**34**:288—97.
27. **Mu YP,** Ogawa T, Kawada N. Reversibility of fibrosis, inflammation and endoplasmic reticulum stress in the liver of rats fed a methionine-choline-deficient diet. *Lab Invest* 2010;**90**:245—56.
28. **Kristensen DB,** Kawada N, Imamura K, *et al.* Proteome analysis of rat hepatic stellate cells. *Hepatology* 2000;**32**:268—77.
29. **Xu L,** Hui AY, Albanis E, *et al.* Human hepatic stellate cell lines, LX-1 and LX-2: new tools for analysis of hepatic fibrosis. *Gut* 2005;**54**:142—51.
30. **Ogawa T,** Iizuka M, Sekiya Y, *et al.* Suppression of type I collagen production by microRNA-29b in cultured human stellate cells. *Biochem Biophys Res Commun* 2010;**391**:316—21.
31. **Sekiya Y,** Ogawa T, Iizuka M, *et al.* Down-regulation of cyclin E1 expression by microRNA-195 accounts for interferon-beta-induced inhibition of hepatic stellate cell proliferation. *J Cell Physiol* 2011;**226**:2535—42.
32. **Murakami Y,** Toyoda H, Tanaka M, *et al.* The progression of liver fibrosis is related with overexpression of the miR-199 and 200 families. *PLoS One* 2011;**6**:e16081.
33. **Galardi S,** Mercatelli N, Farace MG, *et al.* NF-kB and c-Jun induce the expression of the oncogenic miR-221 and miR-222 in prostate carcinoma and glioblastoma cells. *Nucleic Acids Res* 2011;**39**:3892—902.
34. **Lee KS,** Buck M, Houglum K, *et al.* Activation of hepatic stellate cells by TGF alpha and collagen type I is mediated by oxidative stress through c-myb expression. *J Clin Invest* 1995;**96**:2461—8.
35. **Rippe RA,** Schrum LW, Stefanovic B, *et al.* NF-kappaB inhibits expression of the alpha1(I) collagen gene. *DNA Cell Biol* 1999;**18**:751—61.
36. **Lang A,** Schoonhoven R, Tuvia S, *et al.* Nuclear factor kappaB in proliferation, activation and apoptosis in rat hepatic stellate cells. *J Hepatol* 2000;**33**:49—58.
37. **Fornari F,** Gramantieri L, Ferracin M, *et al.* MiR-221 controls CDKN1C/p57 and CDKN1B/p27 expression in human hepatocellular carcinoma. *Oncogene* 2008;**27**:5651—61.
38. **Roderburg C,** Urban GW, Bettermann K, *et al.* Micro-RNA profiling reveals a role for miR-29 in human and murine liver fibrosis. *Hepatology* 2011;**53**:209—18.
39. **Yoshida H,** Shiratori Y, Moriyama M, *et al.* Interferon therapy reduces the risk for hepatocellular carcinoma: national surveillance program of cirrhotic and noncirrhotic patients with chronic hepatitis C in Japan. IHIT Study Group. Inhibition of Hepatocarcinogenesis by Interferon Therapy. *Ann Intern Med* 1999;**131**:174—81.
40. **Garofalo M,** Di Leva G, Romano G, *et al.* miR-221&222 regulate TRAIL resistance and enhance tumorigenicity through PTEN and TIMP3 downregulation. *Cancer Cell* 2009;**16**:498—509.
41. **le Sage C,** Nagel R, Egan DA, *et al.* Regulation of the p27(Kip1) tumor suppressor by miR-221 and miR-222 promotes cancer cell proliferation. *Embo J* 2007;**26**:3699—708.
42. **Galardi S,** Mercatelli N, Giorda E, *et al.* miR-221 and miR-222 expression affects the proliferation potential of human prostate carcinoma cell lines by targeting p27Kip1. *J Biol Chem* 2007;**282**:23716—24.
43. **Kosaka N,** Iguchi H, Ochiya T. Circulating microRNA in body fluid: a new potential biomarker for cancer diagnosis and prognosis. *Cancer Sci* 2010;**101**:2087—92.
44. **Li J,** Wang Y, Yu W, *et al.* Expression of serum miR-221 in human hepatocellular carcinoma and its prognostic significance. *Biochem Biophys Res Commun* 2011;**406**:70—3.

Biochemical and Biophysical Research Communications 412 (2011) 74–79

Contents lists available at ScienceDirect

Biochemical and Biophysical Research Communications

journal homepage: www.elsevier.com/locate/ybbrc

Suppression of hepatic stellate cell activation by microRNA-29b

Yumiko Sekiya [a,b], Tomohiro Ogawa [a,b,1], Katsutoshi Yoshizato [a,b,c], Kazuo Ikeda [d], Norifumi Kawada [a,b,*]

[a] Department of Hepatology, Graduate School of Medicine, Osaka City University, Osaka, Japan
[b] Liver Research Center, Graduate School of Medicine, Osaka City University, Osaka, Japan
[c] PhoenixBio Co. Ltd., Hiroshima, Japan
[d] Department of Anatomy and Cell Biology, Graduate School of Medical Sciences, Nagoya City University, Aichi, Japan

ARTICLE INFO

Article history:
Received 6 July 2011
Available online 26 July 2011

Keywords:
α-Smooth muscle actin
c-fos
Focal adhesion kinase
Extracellular signal-regulated kinase
Akt
Liver fibrosis

ABSTRACT

MicroRNAs (miRNAs) participate in the regulation of cellular functions including proliferation, apoptosis, and migration. It has been previously shown that the miR-29 family is involved in regulating type I collagen expression by interacting with the 3′UTR of its mRNA. Here, we investigated the roles of miR-29b in the activation of mouse primary-cultured hepatic stellate cells (HSCs), a principal collagen-producing cell in the liver. Expression of miR-29b was found to be down-regulated during HSC activation in primary culture. Transfection of a miR-29b precursor markedly attenuated the expression of Col1a1 and Col1a2 mRNAs and additionally blunted the increased expression of α-SMA, DDR2, FN1, ITGB1, and PDGFR-β, which are key genes involved in the activation of HSCs. Further, overexpression of miR-29b led HSCs to remain in a quiescent state, as evidenced by their quiescent star-like cell morphology. Although phosphorylation of FAK, ERK, and Akt, and the mRNA expression of c-jun was unaffected, miR-29b overexpression suppressed the expression of c-fos mRNA. These results suggested that miR-29b is involved in the activation of HSCs and could be a candidate molecule for suppressing their activation and consequent liver fibrosis.

1. Introduction

Liver fibrosis is characterized by excessive accumulation of extracellular matrices (ECMs) and is a common feature of chronic liver injury. Hepatic stellate cells (HSCs) are considered to be the primary population that contributes to fibrogenic reactions by producing ECM in response to liver trauma. HSCs, which reside in the space of Disse outside the liver sinusoids, maintain a quiescent phenotype and store vitamin A under physiological conditions. When liver injury occurs, they become activated and trans-differentiate into myofibroblast-like cells, which are proliferative cells that lose their vitamin A droplets, express α-smooth muscle actin (α-SMA), and secrete profibrogenic mediators and ECM proteins [1,2]. Therefore, controlling the activation of the HSC population is considered a potential therapeutic target for liver fibrosis.

MicroRNAs (miRNAs) are endogenous, small, non-coding RNAs that work as post-transcriptional regulators of gene expression through their interaction with the 3′ untranslated region (3′UTR) of target mRNAs [3]. They participate in various biological phenomena, such as cell proliferation, development, differentiation, and metabolism [3]. Regarding HSCs, it was reported that miR-15b and miR-16 are down-regulated upon HSC activation and that their overexpression induces apoptosis and a delay in the cell cycle progression of HSCs [4,5]. Knockdown of miR-27a and miR-27b in activated HSCs reportedly allowed their reversion to a quiescent phenotype and decreased their rate of cell proliferation [6]. MiR-150 and miR-194 were reported to suppress proliferation, activation, and ECM production by HSCs [7]. We also reported the involvement of miR-195 in the proliferation of HSCs when treated with interferon [8].

Previously, we showed that miR-29b was induced by interferon treatment and that it suppressed type I collagen production in the human HSC line LX-2 [9]. Moreover, Roderburg et al. reported that miRNAs in the miR-29 family were significantly decreased in the

Abbreviations: BSA, bovine serum albumin; Col1a1, alpha 1 (I) collagen; Col1a2, alpha 2 (I) collagen; DDR, discoidin domain receptor; DAPI, 4′,6-diamidino-2-phenylindole; DMEM, Dulbecco's modified Eagle's medium; ECM, extracellular matrix; ERK, extracellular signal-regulated kinase; FAK, focal adhesion kinase; FBS, fetal bovine serum; FN, fibronectin; GAPDH, glyceraldehyde-3-phosphate dehydrogenase; HSC, hepatic stellate cell; ITGB1, integrin β1; miRNA, microRNA; PBS, phosphate buffered saline; PDGFR-β, platelet-derived growth factor receptor-β; PI3K, phosphatidylinositol-3 kinase; SDS, sodium dodecyl sulfate; α-SMA, α-smooth muscle actin; TGF-β, transforming growth factor-β; 3′UTR, 3′ untranslated region.

* Corresponding author. Address: Department of Hepatology, Graduate School of Medicine, Osaka City University, 1-4-3 Asahimachi, Abeno, Osaka 545-8585, Japan. Fax: +81 6 6646 6072.
E-mail address: kawadanori@med.osaka-cu.ac.jp (N. Kawada).
[1] Present address: Center for the Advancement of Higher Education, Faculty of Engineering, Kinki University, Hiroshima, Japan.

0006-291X/$ - see front matter © 2011 Elsevier Inc. All rights reserved.
doi:10.1016/j.bbrc.2011.07.041

fibrotic liver tissue of humans and mice [10]. Thus, it has been speculated that the change in the expression of miR-29 is closely related to the development of liver fibrosis. Although analyses of miR-29 functions were performed on ECM metabolism in these reports, the cells used in these experiments were immortalized cell lines that had already been activated and had become myofibroblastic, which does not always reflect miR-29 function in quiescent HSCs *in vivo*. Therefore, it is important to evaluate the effect of miR-29 on the activation of primary-cultured HSCs. These cells are known to undergo spontaneous activation and transdifferentiation into myofibroblastic cells in culture, similarly to those *in vivo*. Activated HSCs express α-SMA and produce fibrogenic mediators, such as type I collagen and transforming growth factor-β (TGF-β).

Here, we show the effects of miR-29b on the activation of HSCs using freshly isolated primary-cultured mouse HSCs. Overexpression of miR-29b suppressed cell viability and the expression of α-SMA. These effects seemed to be independent of the activation of focal adhesion kinase (FAK), extracellular signal-regulated kinase (ERK), and phosphatidylinositol-3 kinase (PI3K)–Akt, but were partially dependent on the reduction of c-fos mRNA.

2. Materials and methods

2.1. Cells

Primary HSCs were isolated from 12- to 16-week-old male C57BL/6N mice (Japan SLC Inc., Shizuoka, Japan) by pronase–collagenase digestion and subsequent purification by a single-step Nycodenz gradient, as previously described [11]. All animals received humane care, and the experimental protocol was approved by the Committee of Laboratory Animals according to institutional guidelines. Isolated HSCs were cultured on plastic dishes or glass chamber slides in Dulbecco's modified Eagle's medium (DMEM) (Sigma Chemical Co., St. Louis, MO, USA) supplemented with 10% fetal bovine serum (FBS) (Invitrogen, Carlsbad, CA, USA), 100 U/ml penicillin, and 100 μg/ml streptomycin. The purity of cultures was evaluated by observation of the characteristic stellate cell shape using phase-contrast microscopy.

The human HSC line LX-2 was donated by Dr. Scott L. Friedman (Mount Sinai School of Medicine, New York, NY, USA) [12]. LX-2 cells were maintained in DMEM as described above.

2.2. Transient transfection of a miR-29b precursor

The miR-29b precursor (Ambion, Austin, TX, USA), which was a double-strand RNA mimicking the endogenous miR-29b precursor, and a negative control (Ambion) were transfected into mouse HSCs and LX-2 cells using Lipofectamine RNAiMAX (Invitrogen) at a final concentration of 10 nM in accordance with the manufacturer's instructions. Briefly, the miRNA precursor and Lipofectamine RNAiMAX were mixed at a ratio of 5 (pmol):1 (μl) in Opti-MEM I Reduced Medium (Invitrogen), incubated for 20 min at room temperature, and then added to the cultures.

2.3. Quantitative real-time PCR

Total RNA was extracted from cells using the miRNeasy Mini Kit (Qiagen, Valencia, CA, USA). Fifty nanograms of total RNA was reverse-transcribed to cDNA using the ReverTra Ace qPCR RT Kit (Toyobo, Osaka, Japan) in accordance with the manufacturer's instructions. Gene expression was measured by real-time PCR using cDNA, SYBR Green real-time PCR Master Mix (Toyobo), and a set of gene-specific oligonucleotide primers [alpha 1 (I) collagen (Col1a1): forward 5′-CCTGGCAAAGACGGACTCAAC-3′, reverse 5′-GCTGAAGT CATAACCGCCACTG-3′; alpha 2 (I) collagen (Col1a2): forward 5′-AA GGGTCCCTCTGGAGAACC-3′, reverse 5′-TCTAGAGCCAGGGAG AC-CCA-3′; α-SMA: forward 5′-TCCCTGGAGAAGAGCTACGAACT-3′, reverse 5′-AAGCGTTCGTTTCCAATGGT-3′; discoidin domain receptor (DDR) 2: forward 5′-CGAAAGCTTCCAGAGTTTGC-3′, reverse 5′-GCT TCACAACACCACTGCAC-3′; fibronectin (FN) 1: forward 5′-GATGCC GATCAGAAGTTTGG-3′, reverse 5′-GGTTGTGCAGATCTCCTCGT-3′; β1 integrin (ITGB1): forward 5′-CAACCACAACAGCTGCTTCTAA-3′, reverse 5′-TCAGCCCTCTTGAATTTTAATGT-3′; platelet-derived growth factor receptor-β (PDGFR-β): forward 5′-GCGTATCTATATCT TTGTGCCAGA-3′, reverse 5′-ACAGGTCCTCGGAG TCCAT-3′; c-fos: forward 5′-AGAAGGGGCAAAGTAGAGCA-3′, reverse 5′-CAGCTCC CTCCTCCGATT-3′; c-jun: forward 5′-CCAGAAGATGGTGTGGTGTTT-3′, reverse 5′-CTGACCCTCTCCCCTTGC-3′; glyceraldehyde-3-phosphate dehydrogenase (GAPDH): forward 5′-TGCACCACCAACTGCT-TAG-3′, reverse 5′-GGATGCAGGGATGATGTTC-3′] using an Applied Biosystems Prism 7500 (Applied Biosystems, Foster City, CA, USA). To detect miR-29b expression, the reverse transcription reaction was performed using a TaqMan microRNA Assay (Applied Biosystems) in accordance with the manufacturer's instructions. The expression level of GAPDH was used to normalize the relative abundance of mRNAs and miR-29b.

2.4. Immunoblots

Cells were lysed in RIPA buffer [50 mM Tris/HCl, pH7.5, 150 mM NaCl, 1% NP-40, 0.5% sodium deoxycholate, 0.1% sodium dodecyl sulfate (SDS)] containing Protease Inhibitor Cocktail, Phosphatase Inhibitor Cocktail 1, and Phosphatase Inhibitor Cocktail 2 (Sigma). Proteins (2.5–10 μg) were electrophoresed in a 5–20% gradient SDS–polyacrylamide gel (ATTO Co., Tokyo, Japan) and were then transferred onto Immobilon P membranes (Millipore, Bedford, MA, USA). After blocking, the membranes were incubated with primary antibodies [mouse monoclonal antibody against α-SMA (Dako, Ely, UK); rabbit polyclonal antibody against type I collagen (Rockland Immunochemicals, Inc., Gilbertsville, PA, USA); rabbit polyclonal antibodies against PDGFR-β and GAPDH (Santa Cruz Biotechnology Inc., Santa Cruz, CA, USA); rabbit polyclonal antibodies against FAK and phospho-FAK (Y397) (Cell Signaling Technology Inc., Beverly, MA, USA); and mouse monoclonal antibodies against ERK, phospho-ERK (T202/Y204), Akt, and phospho-Akt (S473) (Cell Signaling Technology Inc.)] followed by peroxidase-conjugated secondary antibodies (Dako). Immunoreactive bands were visualized by the enhanced chemiluminescence system (Amersham, Roosdaal, Netherlands) using a Fujifilm Image Reader LAS-3000 (Fuji Medical Systems, Stamford, CT, USA).

2.5. F-actin staining

HSCs on glass chamber slides were fixed in 4% paraformaldehyde in phosphate buffered saline (PBS) for 30 min and were permeabilized with 0.1% Triton X-100 in PBS for 5 min at room temperature. The nonspecific background signal was blocked with 1% bovine serum albumin (BSA) in PBS for 20 min. F-actin was stained with MFP488-phalloidin (Mobitec, Goettingen, Germany) in PBS with 1% BSA for 20 min. 4′,6-diamidino-2-phenylindole (DAPI) (Dojindo Laboratories, Kumamoto, Japan) was used for counterstaining.

2.6. Cell viability assay

The cell viability was evaluated by the WST-1 assay based changes in absorbance at 450 nm. Freshly isolated mouse HSCs or LX-2 cells were plated in 96-well plates at a density of 1.5×10^4 or 3×10^3 cells/well, respectively. The following day, cells were transfected with the miR-29b precursor or a negative

control as described above and were incubated for an additional 3 or 5 days before the assessment of cell viability. In another experiment, mouse HSCs that were transfected with the miR-29b precursor the day before were serum-starved overnight and then stimulated with PDGF-BB (10 ng/ml) (R&D Systems, Minneapolis, MO, USA). After incubation for 3 days, cell viability was assessed by the WST-1 assay.

2.7. Statistical analysis

Data presented as bar graphs are the means ± SD of at least three independent experiments. Statistical analysis was performed using the Student's *t*-test, and $P < 0.05$ was considered to be statistically significant.

3. Results and discussion

3.1. Expression of miR-29b in mouse HSCs during spontaneous activation

At 1 day of culture after isolation, mouse HSCs adhered to plastic plates and exhibited round cell bodies with numerous lipid droplets similar to those observed in lipocytes (Fig. 1A). Cell bodies then began to gradually spread and flatten, increasing in size, and losing lipid droplets, resulting in the activated myofibroblastic phenotype (Fig. 1A). In addition to the changes in cell appearance, mRNA expression levels of α-SMA, Col1a1, Col1a2, FN1, DDR2, ITGB1, and PDGFR-β significantly increased at Days 4 and 7 of culture as compared to Day 1 (Fig. 1B). Immunoblot analyses confirmed the increases of type I collagen, α-SMA, and PDGFR-β protein levels at Days 4 and 7 (Fig. 1C). These molecules have already been reported to be up-regulated in activated HSCs and involved in fibrosis [2]. Thus, the primary mouse HSCs used in this study were in an activated state. Although TGF-β1 is known as a key regulator of collagen production and fibrosis [13], its mRNA expression level in mouse HSCs remained unchanged due to an unknown reason in this study (Fig. 1B). In contrast, miR-29b expression in mouse HSCs was significantly decreased to 28% and 32% at Days 4 and 7, respectively, as compared to Day 1 (Fig. 1D). These findings raised the possibility that a reduction in miR-29b contributed to the up-regulation of the fibrosis-related genes listed above.

3.2. Effects of miR-29b overexpression on the activation of HSCs

To investigate this possibility, we next examined the effects of miR-29b overexpression on the activation of HSCs. Overexpression of miR-29b was achieved by the transient transfection of a synthesized miR-29b precursor, which was a double-strand RNA mimicking the endogenous miR-29b precursor. As shown in Fig. 2A, transfection of the miR-29b precursor markedly suppressed mRNA expression of Col1a1 and Col1a2 to 8% and 18%, respectively. Transfection significantly reduced mRNA expression of FN1 to 61% and also affected the expression of HSC activation-related molecules, such as α-SMA, DDR2, ITGB1, and PDGFR-β to 57%, 62%, 73%, and

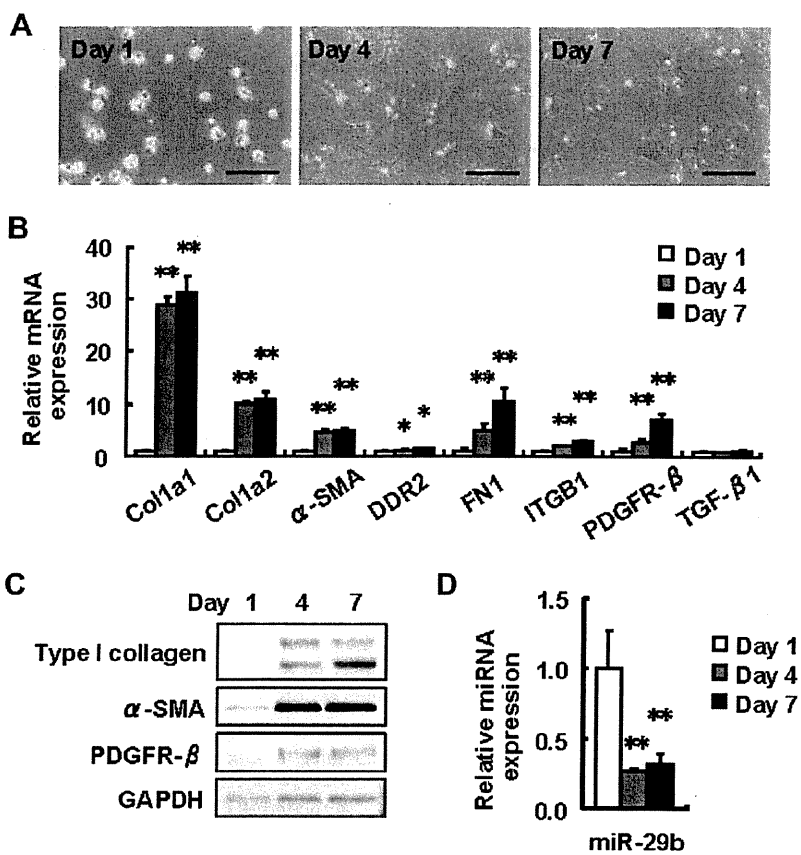

Fig. 1. Expression of miR-29b in mouse primary HSCs during culture. HSCs were isolated from mouse liver (Day 0) and cultured for the indicated periods. (A) Phase-contrast microscopy. Scale bar, 200 μm. (B) mRNA expression levels of Col1a1, Col1a2, α-SMA, DDR2, FN1, ITGB1, PDGFR-β and TGF-β1 were analyzed by real-time PCR. Results are expressed as relative expression against the expression on Day 1 of corresponding genes. $^{*}P < 0.05$, $^{**}P < 0.01$ compared with Day 1. (C) Protein expression levels of type I collagen, α-SMA and PDGFR-β were analyzed by Western blot. GAPDH served as an internal control. (D) miR-29b expression level was analyzed by real-time PCR. $^{*}P < 0.05$, $^{**}P < 0.01$ compared with Day 1.

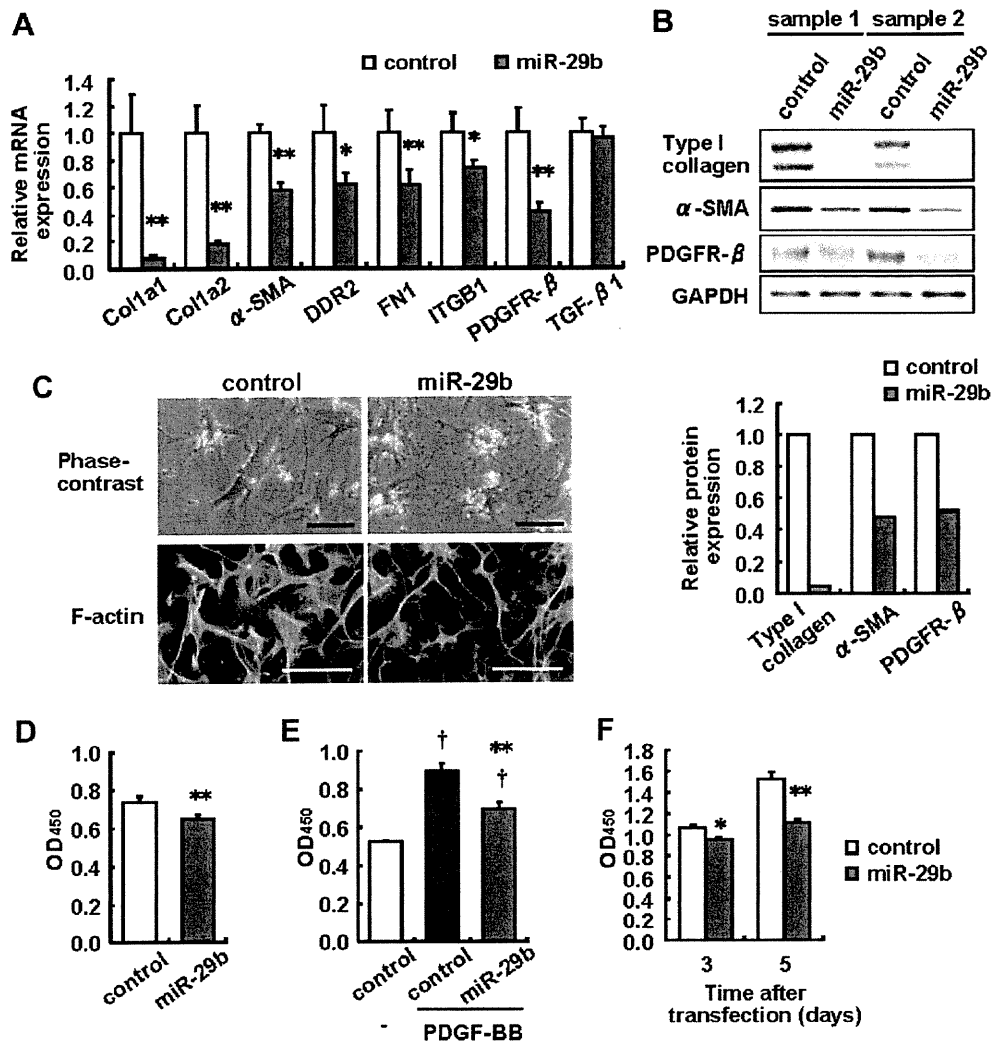

Fig. 2. Effects of miR-29b overexpression on the activation of HSCs. (A–D) Mouse HSCs were transfected with 10 nM miR-29b precursor or a negative control (control) on Day 1 and incubated for 3 days. (A) mRNA expression levels of Col1a1, Col1a2, α-SMA, DDR2, FN1, ITGB1, PDGFR-β and TGF-β1 were analyzed by real-time PCR. The results are expressed as relative expression against the expression of untreated control. $^{*}P < 0.05$, $^{**}P < 0.01$ compared with control. (B) Protein expression levels of type I collagen, α-SMA and PDGFR-β were analyzed by Western blot. GAPDH served as an internal control. The lower graph indicates the densitometric results of $n = 2$. (C) Phase-contrast microscopy (upper) and MFP488-phalloidin staining for F-actin (lower). Scale bar, 100 μm. (D) Cell viability was evaluated by WST-1 assay. $^{**}P < 0.01$ compared with control. (E) Mouse HSCs were transfected with miR-29b precursor or a negative control (control) on Day 1. Twenty-four hours later, cells were serum-starved overnight, stimulated with or without PDGF-BB (10 ng/ml) and incubated for an additional 3 days. In Day 6, cell viability was evaluated by WST-1 assay. $^{**}P < 0.01$ compared with control plus PDGF-BB. $^{\dagger}P < 0.05$ compared with control plus non-treat. (F) LX-2 cells were transfected with miR-29b precursor or a negative control (control) and incubated for the indicated periods. Cell viability was evaluated by WST-1 assay. $^{*}P < 0.05$, $^{**}P < 0.01$ compared with the control.

42%, respectively. The TGF-β1 mRNA level was unaffected. At the protein level, expression of type I collagen, α-SMA, and PDGFR-β was suppressed by the overexpression of the miR-29b precursor (Fig. 2B). Col1a1, Col1a2, ITGB1, and PDGFR-β are predicted targets of miR-29b according to the miRNA target prediction databases TargetScan (http://www.targetscan.org/), miRBase (http://www.mirbase.org/), and mircrorna.org (http://www.microrna.org). Therefore, the suppression of these proteins might be due to the direct interaction of miR-29b with the 3′UTR of their corresponding mRNAs. Although α-SMA, DDR2, and FN1 are not predicted targets of miR-29b, their mRNA levels were suppressed. Thus, this effect was thought to be a secondary action of miR-29b over-expression. That is, it is suggested that miR-29b can not only target Col1a1, Col1a2, ITGB1, and PDGFR-β, but can also suppress the activation of HSCs by regulating other unidentified mechanisms, resulting in the suppression of α-SMA, DDR2, and FN1. In support of these results, morphological transformation from the quiescent to the myofibroblastic cell shape, as shown in Fig. 1A, was impeded in miR-29b precursor-transfected cells (Fig. 2C); miR-29b precursor-transfected cells exhibited star-like morphology with small cell bodies and slender dendritic processes as compared to negative control-transfected cells at Day 4. Staining with MFP-phalloidin, which labels F-actin, also confirmed cytoskeletal changes in miR-29b precursor-transfected HSCs. Taken together; these results suggest that miR-29b is able to suppress HSC activation as well as ECM expression.

3.3. Effect of miR-29b overexpression on number of HSCs

Activated HSCs are known to acquire proliferation abilities [1,2]. We considered the possibility that miR-29b was able to regulate the number of HSCs. As shown by the WST-1 assay, when the miR-29b precursor was transfected into HSCs at Day 1, the cell number observed at Day 4 was significantly reduced to 88% of the negative control-transfected cells (Fig. 2D). Treatment of HSCs with 10 ng/mL PDGF-BB, a key mitogen for HSCs [14], significantly